An investigation of the thermal neutron cross-section for the reaction N(14)(n,p)C(14) using a nuclear emulsion technique.

Gowing, Richard Maxwell

Pennsylvania State University

AN INVESTIGATION OF THE THERMAL NEUTRON CROSS-SECTION FOR THE REACTION $N^{14}(n,p)C^{14}$ USING A NUCLEAR EMULSION TECHNIQUE

RICHARD MAXWELL GOWING

The Pennsylvania State University

The Graduate School

Department of Physics

An Investigation of the Thermal Neutron Cross-Section for the Reaction $N^{14}(n, p)C^{14}$ Using a Nuclear Emulsion Technique

A thesis in

Physics

by

Lieutenant Richard Maxwell Gowing, USN

Submitted in partial Fulfillment
of the requirements
for the degree of

Master of Sciences

June 1961

Approved:

_____

_____
Associate Professor of Physics,
Thesis Adviser.

_____

_____
Head of the Department of Physics

ACKNOWLEDGMENTS

The author gratefully acknowledges the advice, guidance, and encouragement kindly given to him by Dr. W. W. Pratt throughout the course of this investigation.

Appreciation is expressed to Dr. R. R. Roy for many useful discussions and comments and to the staff of The Pennsylvania State University Research Reactor for their assistance in this investigation.

This work was undertaken through the sponsorship of the U. S. Naval Postgraduate School, Monterey, California and was supported in part by the U. S. Atomic Energy Commission.

TABLE OF CONTENTS

	Page
Acknowledgments	ii
List of Tables	v
List of Figures	vi
I. INTRODUCTION	1
II. THEORETICAL BACKGROUND	4
Development of the working equation for the determination of cross-sections by nuclear emulsion techniques	4
Discussion of the theoretical factors influencing the design of experimental equipment	5
Neutron flux	6
Charged particle flux	10
Gamma ray dose rate	14
Optimum exposure times and distances	19
III. EQUIPMENT AND EXPERIMENTAL PROCEDURE	20
Equipment	20
Fabrication of target plates	22
Description of nuclear emulsions used	25
Experimental geometry	26
Exposure of the nuclear emulsions at The Pennsylvania State University Research Reactor	28
Processing of the nuclear emulsions	
Microscope technique used in reading nuclear emulsions	32
IV. EXPERIMENTAL RESULTS	36
Preliminary results of individual exposures	36
Plate 1	36
Plates 2 and 3	37
Plates 4, 5, and 6	38
Plates 7 and 8	40
Plate 9	41
Plates 10A and 10B	42
Plate 11	44
Plate 12	44
Plate 13	44
Plates 14 and 15	45
Plates 16 and 17	46
Final results of the investigation of the thermal neutron cross-section of the $N^{14}(n, p)C^{14}$ reaction	46

TABLE OF CONTENTS (Continued)

Final results of the investigation of the thermal neutron cross-section of the $N^{14}(n, p)C^{14}$ reaction 46
Discussion of the errors involved in the determination of the upper limit to the $N^{14}(n, p)C^{14}$ cross-section 49
Error in the value used for the cross-section of the $Li^{6}(n, \alpha)H^{3}$ reaction . . . 50
Error of the value used for the natural abundance of Li^{6} and N^{14} 50
Random errors in the numbers of tracks counted 51
Error in N_t^1 and in $N_p^1 + N_{sb}^1$ because of errors in the numbers of tracks counted. 51
Error in the computed value of the upper limit of the $N^{14}(n, p)C^{14}$ cross-section. . 52
Errors arising as a result of the experimental technique 53

V. SUMMARY AND CONCLUSIONS 55

Summary. 55

Comments on the use of nuclear emulsion techniques 56

Suggestions for the refinement of the technique used in this investigation and for further research 56

BIBLIOGRAPHY. 59

LIST OF TABLES

Table 1. Tabulation of thermal neutron cross-sections of nitrogen 2

Table 2. Characteristics of target plates used in the investigation 24

Table 3. Data on exposures made during $N^{14}(n, p)C^{14}$ cross-section investigation 31

LIST OF FIGURES

Figure 1.	Diagram used to illustrate the calculation of the neutron flux at a point on the axis of a plane circular source	7
Figure 2.	Thermal neutron flux at an axial point as a function of distance from a plane circular source of diameter 3.5" and whose initial flux is 1.8×10^9 neutrons/cm^2 sec	9
Figure 3.	A plot of the pressure necessary to insure that a 1.847 Mev alpha particle does not lose more than .205 Mev in passing from the target to the emulsion as a function of the separation of emulsion and target	15
Figure 4.	Gamma ray dose rate for the Pennsylvania State University Research Reactor as a function of the distance in water from the center of the thermal column at reactor power of 200 kw	16
Figure 5.	Maximum time of plate exposure as a function of distance in water between the emulsion and the center of the thermal column face	17
Figure 6.	The number of neutrons/cm^2 passing through a target during the maximum exposure time as a function of the distance of the target from the center of the thermal column face	18
Figure 7.	Cutaway sketch of the nuclear emulsion exposure chamber assembly	21
Figure 8.	(a) Lead shield insert for nuclear emulsion exposure chamber. (b) Cadmium liner for lead shield.	23
Figure 9.	System geometry for exposure of nuclear emulsions	27
Figure 10.	Equipment arrangement during exposure of nuclear emulsions	29
Figure 11.	Sketch of a microscope field of view illustrating the criteria used in track counting	34

LIST OF FIGURES (continued)

Figure 12. Sketch illustrating (a) plate arrangement for exposure 10, (b) section XX - lead shielding removed for exposures 11 and 12, and (c) section YY - lead shielding removed for exposures 13, 14, and 15. 43

I. INTRODUCTION

Among the myriad of possible thermal neutron reactions, there are many, such as $K^{40}(n, p)$ ($\sigma < 1$ barn) and $S^{32}(n,\alpha)$, ($\sigma = (1.8 \pm 1.0) \times 10^{-3}$ barn), which give a charged particle as one of the products of the reaction and for which the cross-section is known only to the extent that it is less than some value or, at best, known only to a fairly low degree of accuracy.[1] This investigation deals with the problem of developing a nuclear emulsion technique to permit the measurement of this type of cross-section to a higher degree of accuracy.

The problem has previously been studied by A. R. Sattler.[2] His nuclear emulsion technique was applied to the study of the thermal neutron cross-section of the $N^{14}(n, p)C^{14}$ reaction. He exposed a lithium loaded nuclear emulsion and an unloaded emulsion (containing nitrogen as one of its constituents) to a thermal neutron flux. By comparing the number of alpha-triton tracks per unit volume in the lithium loaded plate to the number of proton tracks in the unloaded plate, he was able to determine the $N^{14}(n, p)C^{14}$ cross-section relative to the well-known cross-section of the $Li^{6}(n, \alpha)H^{3}$ reaction.

Since the cross-section is relatively small and known to within five percent, the thermal neutron n-p reaction of nitrogen lends itself well to the initial work in the development of methods for determining small cross-sections. Table 1 is a tabulation of the cross-section of nitrogen as reported by other investigators with an indication of the method used in their determinations. Since not all of

Table 1. TABULATION OF THERMAL NEUTRON CROSS-SECTIONS OF NITROGEN

Investigator	Reported Cross-section	Standard	Method of Investigation	Corrected Cross-Section
C. La Pointe and F. Rasetti[4]	1.2 ± .3 b	Boron (600 b)	Thermal neutron density comparison in solutions of boric acid and NH_4NO_3	1.5 ± 4 b
H. Lichtenberger, H. Fowler and A. Wattenberg[5]	1.75 ± .05	Boron (703 b)	Pile Neutron, P. T.	1.78 ± .05
J. H. Coon and R. A. Nobles[6]	1.76 ± .05	Boron (703 b)	Pile Neutron, P. T.	1.89 ± .05
F. O. Colmer and D. Littler[7]	1.76 ± .05	Boron (710 b)	Pile Neutron, P. T.	1.79 ± .05
H. Pomerance[8]	1.86 ± .093	Gold (95 b)	Pile Neutron, P. T.	1.85 ± .10
A. R. Sattler[2]	1.15 ± .05	Lithium (71 b)	Nuclear Emulsions	1.15 ± .05

Note: a) Values in parentheses under Standard are values of the cross-sections used by the investigator.
b) P. T. under Method of investigation means Pulse Technique.
c) The corrected cross-section was obtained by first correcting the reported cross-section in accord with the latest value of the cross-section for the standard used (for boron the latest value is 755 b, for gold 98.8, and lithium 71[1]) and then subtracting the .08 γ cross-section as measured by Bartholomew and Campion.[3]

the investigators studied the same cross-section (some studying the total absorption cross-section and others the n-p cross-section alone) and since the value of the standard used depended on that which was available to the investigator at the time of reporting, the last column of Table 1 gives that value of the n-p cross-section which is consistent with the reported cross-section after having been adjusted to account for the latest value of the standard used and after subtracting the .08 b n-γ cross-section.[3]

A study of Sattler's work indicated that several possible sources of error were involved in his technique. These were: (a) the necessity for counting some tracks which had very unfavorable dip angles in the emulsion; (b) the necessity for obtaining measurements of emulsion thicknesses which was brought about by having counted the alpha-triton tracks on different plates fromthose used to count proton tracks; and (c) the introduction of background tracks caused by the passage of both fast and thermal neutrons through the recording emulsions.

Since, by changing the exposure technique to eliminate or greatly reduce the above listed difficulties, there was a good chance of improving on the value of the cross-section as obtained by Sattler, this investigation dealt with the specific problem of determining the thermal neutron cross-section of the $N^{14}(n, p)C^{14}$ reaction by exposing a target containing Li^6 (used as a standard) and N^{14} to a thermal neutron beam and recording the tracks of the charged particle products in an emulsion positioned with such geometry as to prevent large dip angles and the exposure of the emulsion to the direct neutron beam.

II. THEORETICAL BACKGROUND

Development of the working equation for the determination of cross-sections by nuclear emulsion techniques

Consider a beam of thermal neutrons passing through a thin target containing two types of atoms. Assume that (a) the target is so thin that all products of any reaction occuring will not be prevented from leaving the target by virtue of having beeen stopped in the target, (b) both types of atoms have some cross-section for thermal neutrons resulting in the production of a charged particle, and (c) the angular distribution of the charged particle products is isotropic since the reactions occur as a result of thermal neutrons. If a nuclear emulsion is now positioned such as to record all charged particles coming from the target in a particular direction, then we may expect that the number of charged particle tracks per unit volume, N_i, of a particular kind recorded in the emulsion will be proportional to the cross-section, σ_i, of the reaction causing that kind, the number of atoms per unit volume, n_i, of the type involved in that reaction, and the natural abundance, I_i, of the particular isotope involved. Inserting a constant, K, of proportionality, we may write,

$$N_i = K \sigma_i n_i I_i \quad . . . . . (1)$$

For this investigation, the two types of atoms used were lithium and nitrogen. These elements were used in the form of the compound $LiNO_3$. The charged particles involved were the protons of the n-p reaction of N^{14} and the alpha particles and tritons of the n-α reaction

of Li^6. Using equation (1) and noting that for each alpha particle produced in the $Li^6(n, \alpha)H^3$ reaction there is also one triton, we may write

$$N_p = K \sigma_{N^{14}} n_N I_{N^{14}} \quad . \quad . \quad . \quad . \quad . \quad . \quad . \quad . \quad . \quad . \quad (2)$$

$$N_{H^3} = K \sigma_{Li^6} n_{Li} I_{Li^6} \quad . \quad . \quad . \quad . \quad . \quad . \quad . \quad . \quad . \quad . \quad (3)$$

Since we are using the known value of the lithium cross-section as a reference, we divide equation (2) by equation (3) and solve for the nitrogen cross-section. Thus

$$\sigma_{N^{14}} = \frac{N_p}{N_{H^3}} \frac{n_{Li}}{n_N} \frac{I_{Li^6}}{I_{N^{14}}} \cdot \sigma_{Li^6} = \frac{Np}{N_{H^3}} \frac{I_{Li^6}}{I_{N^{14}}} \sigma_{Li^6} \quad . \quad . \quad . \quad . \quad . \quad . \quad . \quad (4)$$

Discussion of the theoretical factors influencing the design of experimental equipment

As a preliminary to the discussion of the design of equipment and the development of experimental procedures used in this investigation, it may be well to review those condiderations which led to the specifications in the equipment design. These are: (a) the calculation of the neutron flux available at the target as a function of the distance of the target plate from the center of the thermal column face at the Pennsylvania State University Research Reactor; (b) the calculation of the charged particle flux available at the emulsion as a function of the neutron flux through the target and the distance of the emulsion from the target plate; (c) the calculation of the expected gamma ray dose rate at the emulsion as a function of the distance between the emulsion and the center of the thermal column face; and (d) the determination of the optimum exposure times and distances based on the results of (a) through (c) such that an acceptable number of tracks

per field of view in the microscope might be obtained on a readable plate.

In the following discussion, some of the quantities such as the cross-sectional size of the incident neutron beam will be considered constants which might otherwise have been variables except for having been limited by the availability of materials. These constants are: (a) the diameter of the incident neutron beam, 3.5"; (b) the minimum distance between the face of the thermal column and the center of the target plate, 4"; and (c) the maximum distance between the face of the thermal column and the center of the target plate, 100".

Neutron flux

Consider, as illustrated in Figure 1, a plane circular source of neutrons with radius, p, and flux, ϕ_n. The flux, $\phi_{n'}$, through the target, T, at a perpendicular distance, R, from the source will be given by:

$$\phi_{n'} = \int_0^{2\pi}\int_0^{p_0} \frac{p\,dp\,d\phi}{4\pi r^2} = \frac{\phi_n}{4}\int_0^{p_0} \frac{2p\,dp}{r^2} \quad \ldots\ldots\ldots \quad (5)$$

and since $r^2 = p^2 + R^2$, $\phi_{n'} = \frac{\phi_n}{4}\int_0^{p_0} \frac{2p\,dp}{R^2 + p^2} = \frac{\phi_n}{4} \ln\left(\frac{p^2 + R^2}{R^2}\right)$ . . (6)

If the source had been approximated by a point source the flux at the target would have been

$$\phi_{n'} = \frac{\phi_n\,\pi\,p_0^2}{4\pi R^2} = \frac{\phi_n}{4}\,\frac{p_0^2}{R^2}$$

We shall consider the approximation of the circular source by a point source to be valid whenever the ratio of the flux as calculated

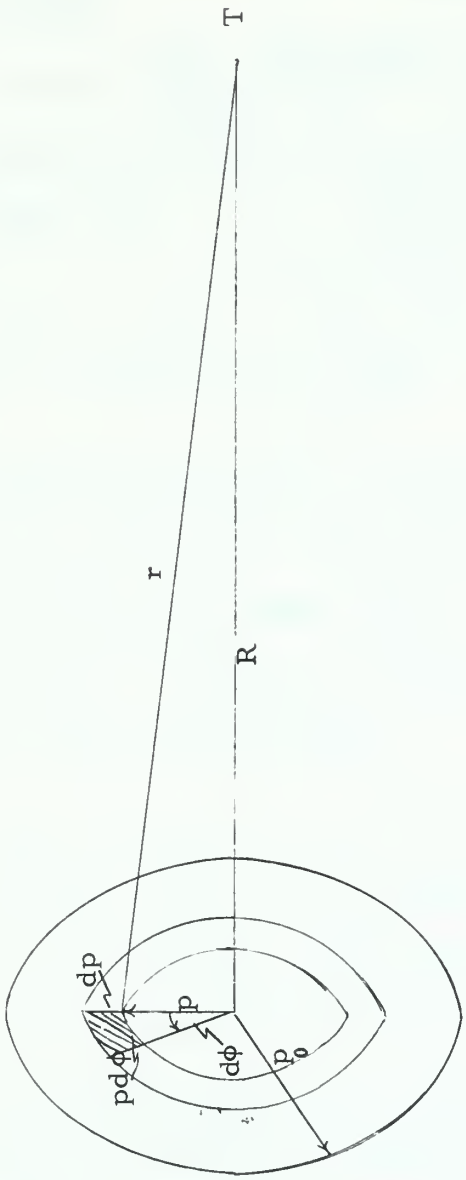

Fig. 1. Diagram used to illustrate the calculation of the neutron flux at a point on the axis of a plane circular source.

in equation (6) is, arbitrarily, at least .9 of the flux as calculated in equation (7), i.e.

$$\frac{\frac{\phi_n}{4}\ln\left(\frac{p_0^2 + R^2}{R^2}\right)}{\frac{\phi_n}{4}\frac{p_0^2}{R^2}} = \frac{R^2}{p_0^2}\ln\left(\frac{p_0^2 + R^2}{R^2}\right) \geq .9 \quad \ldots\ldots \quad (8)$$

Letting $p = f R$, we have $\frac{R^2}{f^2 R^2}\ln\left(\frac{f^2R^2 + R^2}{R^2}\right) = 1/f^2\ln(f^2 + 1) \geq .9$ (9)

Expanding the natural log funciton in a power series gives:

$$1/f^2(f^2 - f^4/2 + f^6/3 - \cdots\cdots) \doteq \frac{2f^4 - 3f^2 + 6}{6} \geq .9 \qquad (10)$$

Hence, $2f^4 - 3f^2 + .6 \geq 0$ and $\left(f^2 - \frac{(3 + 4.2^{1/2})}{4}\right)\left(f^2 - \frac{(3 - 4.2^{1/2})}{4}\right)$ (11)

which is true for $f < 1$ only if $f^2 \leq \frac{3 - 4.2^{1/2}}{4}$ or $f \leq .488$

Based on the results derived above, the approximation is valid whenever the distance of the center of the target is at least 2.05 times the radius of the incident neutron beam. With an incoming neutron beam of 3.5" in diameter, the center of the target must be 3.59" or more from the face of the thermal column.

Figure 2 is a graph showing the flux at the center of the end of a 3.5" diameter tube placed with one end perpendicular to the center of the thermal column face and with the reactor operating at full power (200 kw). The flux is shown as a function of the distance of the point of interest from the thermal column face. The graph is based on an initial flux at the center of the thermal column face of 1.8×10^9 neutrons per square centimeter per second. This value is twice the value found

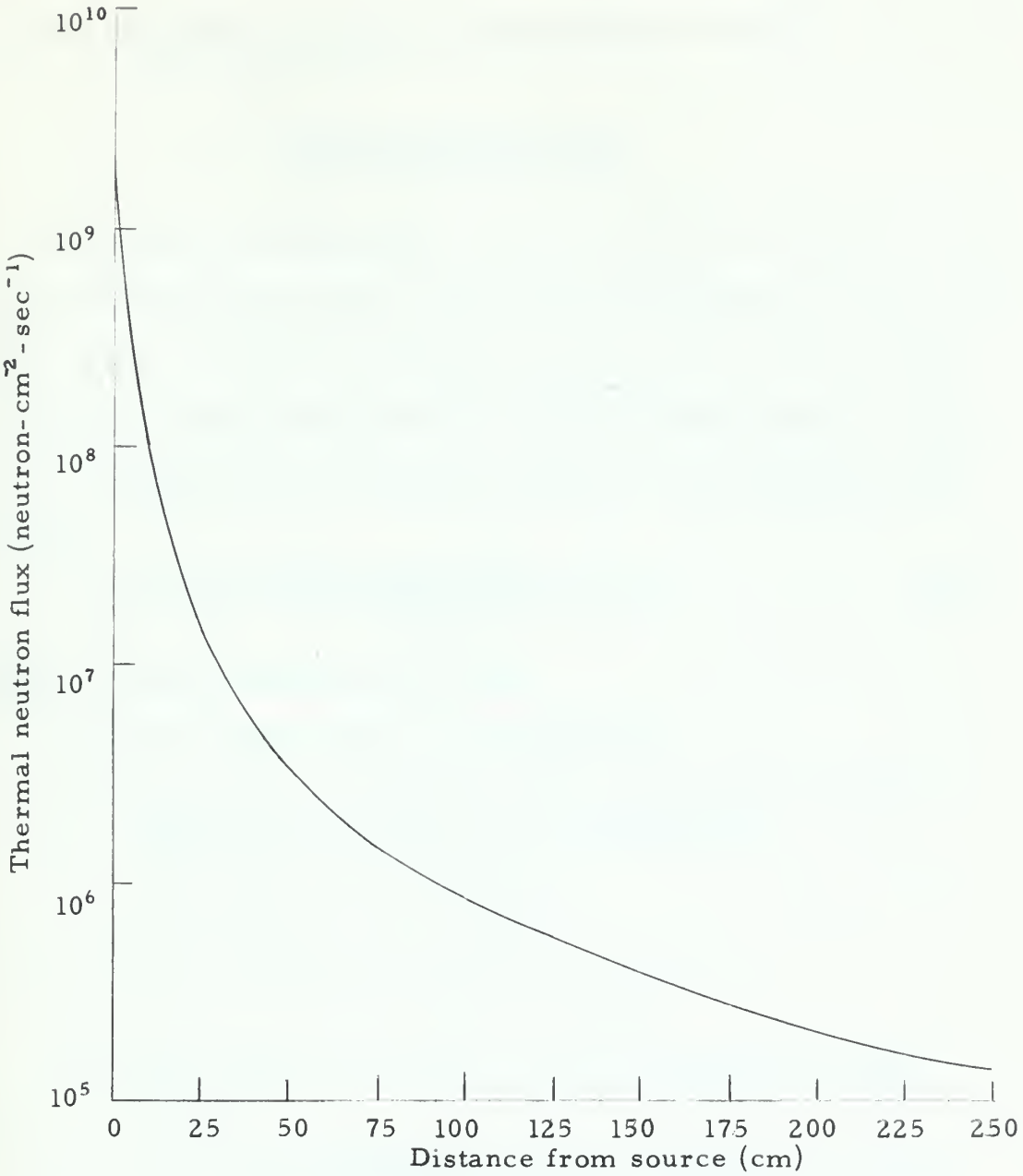

Fig. 2. Thermal neutron flux at an axial point as a function of distance from a plane circular source of diameter 3.5" and whose initial flux is 1.8×10^{9} neutrons-cm^{-2}-sec^{-1}.

by D. E. Kline[8] when the reactor was operating at 100 kw.[9] *

Charged particle flux

For simplicity of discussion, the center of the recording emulsion will be considered to be far enough away from the center of the target plate to make valid the approximation that the source of the charged particles (the target plate) may be considered a point source. The flux of charged particles through the center of the emulsion is then given by:

$$\phi_p = \frac{\phi_{n'} \cos \theta_t \, a_t \, t_t \, \rho_t \, n_i \, I_j \, N_0 \sigma \sin \theta_e}{4\pi R^2 A_t} \qquad (12)$$

where ϕ_p is the charged particle flux

$\phi_{n'}$ is the neutron flux in the target plate

θ_t is the angle of inclination of the target plate to a plane normal to the direction of the neutron beam

a_t is the area of the target plate

t_t is the thickness of the target

ρ_t is the density of the target compound

n_i is the number of ith type atoms per molecule of target compound

I_j is the natural abundance of jth type isotopes in a natural assembly of ith type atoms

N_o is Avagadro's number

---

* A conversation with Mr. E. S. Kenny, Acting Director of The Pennsylvania State University Research Reactor Facility, indicated that the few measurements made of the thermal neutron flux and gamma ray dose rate at the reactor since it was changed to 200 kw full power operation vice 100 kw have indicated that the doubling of Kline's values is a valid assumption.

σ is the cross-section for the reaction giving the charged particle in question

θ_e is the angle of inclination of the emulsion to a plane normal to the direction of the neutron beam

R is the distance of the center of the emulsion from the center of the target

A_t is the gram molecular weight of the target compound

In order to prevent an excessive straggling in range in the recording emulsion, the thickness of the target and the density of air should be such that the energy of the charged particle is not reduced below some reasonable fraction of its original value. Since this investigation dealt with particles whose range in the emulsion was of the order of 5-6 microns and since tracks of a range in the emulsion of less than 4 microns are not easily seen, it is considered reasonable to require that particles entering the emulsion have at least .8 of their original energy. .1 of the original energy would be permitted to be lost in the target material itself and the other .1 could be lost in the particle traversing the air between the target and the emulsion.

The target material to be used in this investigation was $LiNO_3$. The stopping power of $LiNO_3$ was computed by the use of the empirical formula[10]

$$S = -\frac{dE}{dx} = 2\pi e^4 Z^2 \left(\frac{M}{m}\right)_e \frac{1}{E} \frac{\rho N_0}{A} \sum_i n_i Z_i \ln \frac{4Em_e}{I_i M} \quad . \quad . \quad . \quad (13)$$

where S is the stopping power

t is the thickness of the stopping substance

e is the charge on an electron

Z is the atomic number of the incident particle

M is the mass of the incident particle

m_e is the mass of an electron

E is the energy of the incident particle

n_i is the number of atoms of the ith type in the compound

Z_i is the atomic number of the ith type atom

$\bar{I}_i$ is the average excitation potential of atoms of the ith type

ρ is the density of the stopping substance

N_0 is Avagadro's number

A is the molecular weight of the stopping substance

Since the target plate will be inclined at an angle of 45^0 to the neutron beam, the thickness of the target such that the energy of a particle originating at the back of the target (that side which is the furthest from the emulsion) will not be reduced to less than .9 of the original value is given by:

$$t = - \frac{.1\, E_p \cos 45}{\frac{dE}{dx}} \qquad (14)$$

The energies of the alpha particles, tritons, and protons in the $Li^6(n, \alpha)H^3$ and $N^{14}(n, p)C^{14}$ reactions are:

$$Li^6(n, \alpha)H^{3\,11} \quad E_\alpha = 2.052$$

$$E_{H^3} = 2.736$$

$$N^{14}(n, p)C^{14\,12} \quad E_p = 0.584$$

Using the values for the energies as listed above in equations (13) and (14) yields the following values for maximum allowable thicknesses:

.141 mg/cm^2 for alpha particles

1.01 mg/cm^2 for tritons
.175 mg/cm^2 for protons

Therefore, the thickness of the target to be used was chosen to be .141 mg/cm^2 to insure that the energy of no particle originating in the target from a thermal neutron reaction would be reduced below .9 of its original value by virtue of having been slowed down in the target material itself.

Consider alpha particles, tritons, and protons which have originated at the back of the target and have lost .1 of their original energy in traversing the target material. They will have energies of 1.847 2.462, and .526 Mev respectively upon entering air at STP. If the particles are not to enter the emulsion with less than .8 of their original energy, then they must not fall below 1.642, 2.189, and .467 Mev respectively.

The range in air at STP is given by Bethe[10] for alpha particles and protons of various energies; tabulated below are the ranges for the energies of interest in this investigation.

Particle	Energy (Mev)	Range in air (cm)	Difference in range
Alpha	1.847	.92	
	1.642	.82	.10
Proton	.526	.86	
	.467	.73	.13

No data was available on the ranges of tritons in air, however, since the triton is 1 mass unit lighter than the alpha particle and is only singly charged, one assumes that its difference in range for the same percentage decrease in energy would not be less than the .10 cm of the alpha particle noted above. Therefore, the distance between

centers of the target and the recording emulsion should not be more than .10 cm of air at STP to insure that particles do not enter the emulsion with less than .8 of their original energy.

The distance between the target and the emulsion can be made a variable if the system is placed under a vacuum. Assuming that the range of a particle in air is inversely proportional to the density of air and that the density is directly proportional to the pressure, then the vacuum necessary for a given distance between centers is given by:

$$\text{Pressure (atmospheres)} = \frac{\text{Range in air at STP (.10 cm)}}{\text{Distance between centers}}$$

Figure 3 shows a plot of the pressure as a function of the distance between the target and the emulsion for a maximum separation of .10 cm at STP.

Gamma ray dose rate

D. E. Kline[8] has measured the gamma ray dose rate of the Pennsylvania State University Research Reactor as a function of distance in water from the center of the face of the thermal column while the reactor was operating at 100 kw. Figure 4 is taken from Kline's plot by multiplying the dose rates by a factor of two in order that a plot of the dose rate at reactor power 200 kw might be obtained.*

See note on bottom of page 10.

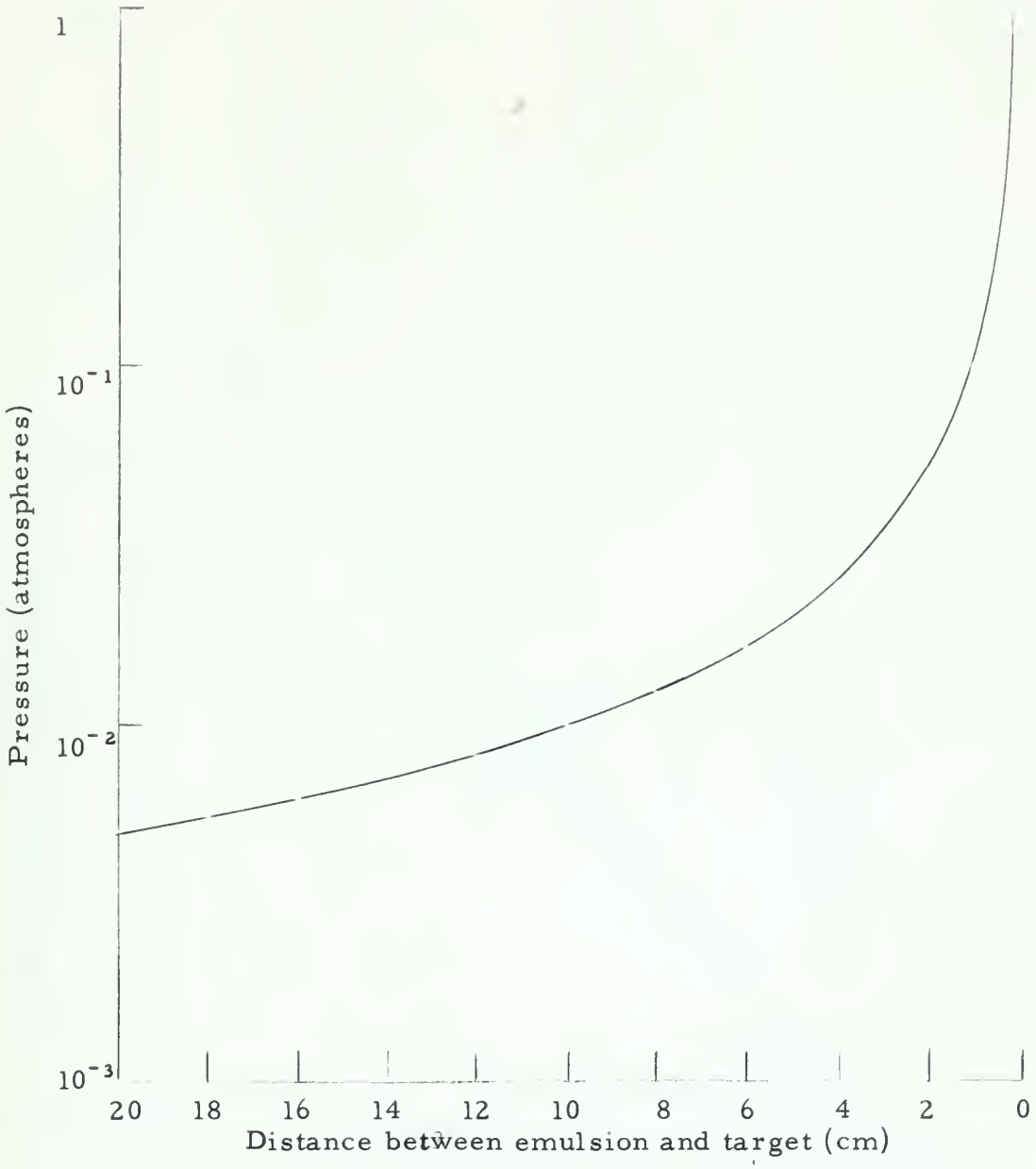

Fig. 3. A plot of the pressure necessary to insure that a 1.847 Mev alpha particle does not lose more than .205 Mev in passing from the target to the emulsion as a function of the separation of emulsion and target.

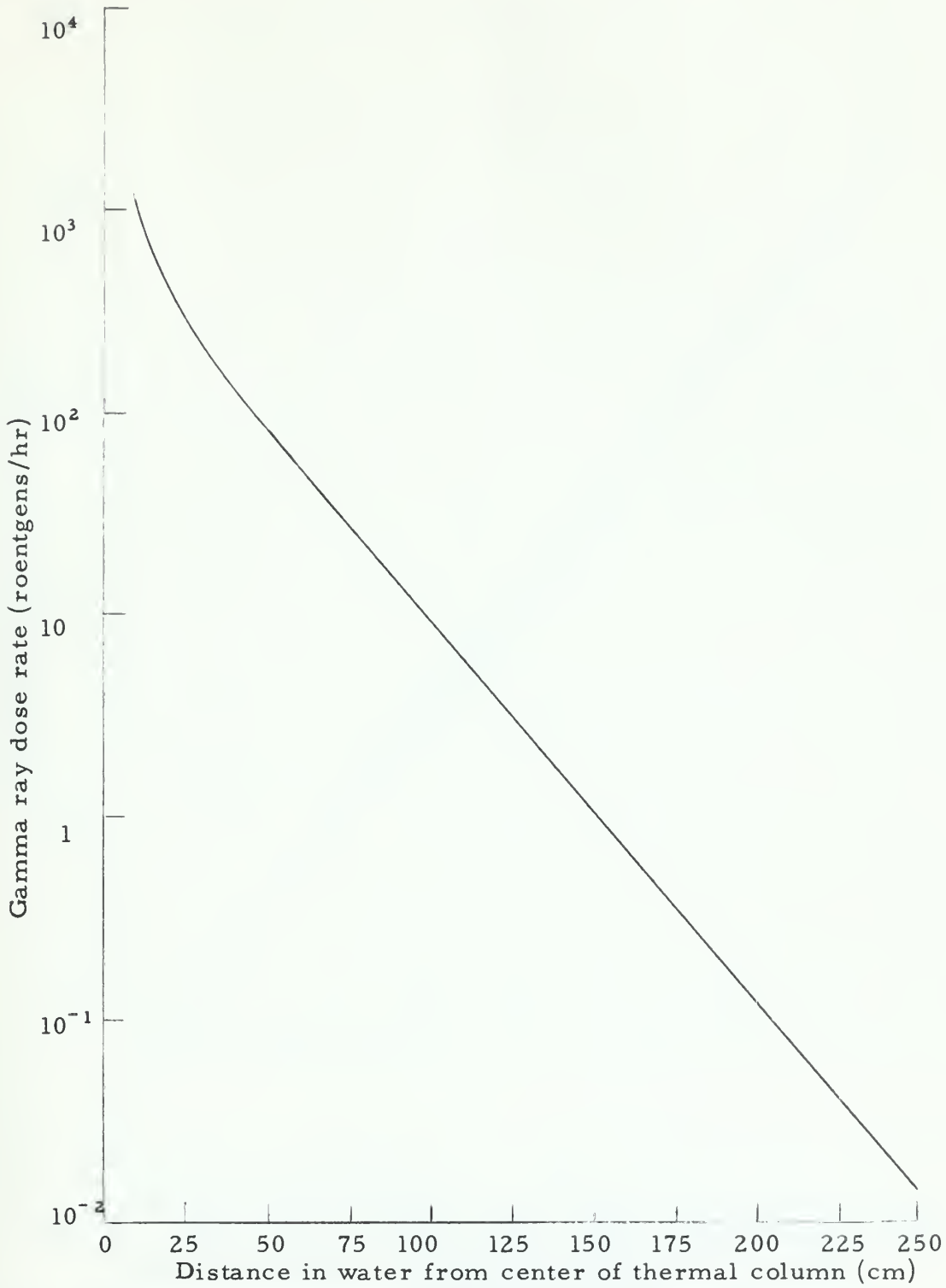

Fig. 4. Gamma ray dose rate for the Pennsylvania State University Research Reactor as a function of the distance in water from the center of the thermal column at reactor power of 200 kw.

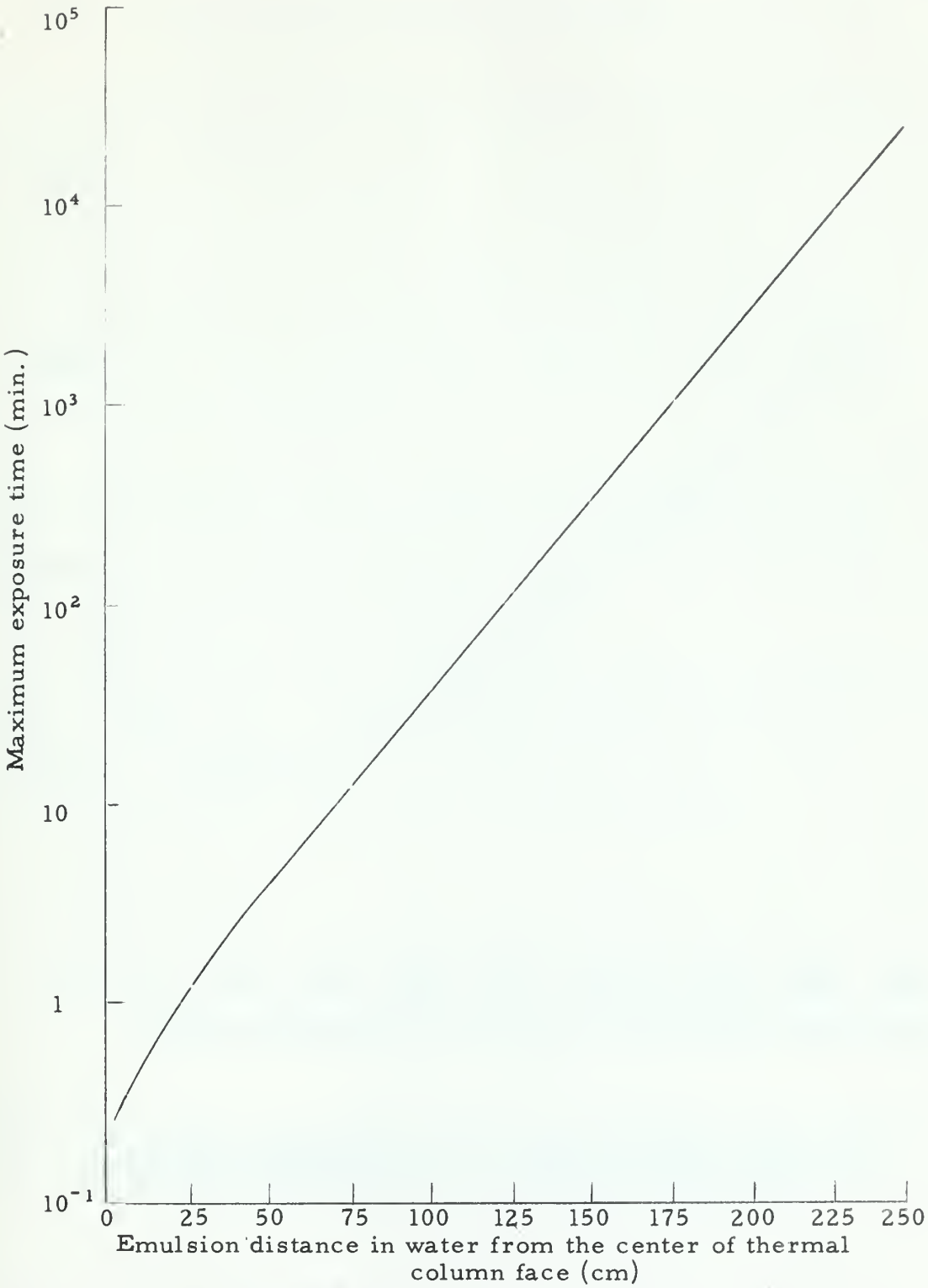

Fig. 5 Maximum time of plate exposure as a function of distance in water between the emulsion and the center of the thermal column face.

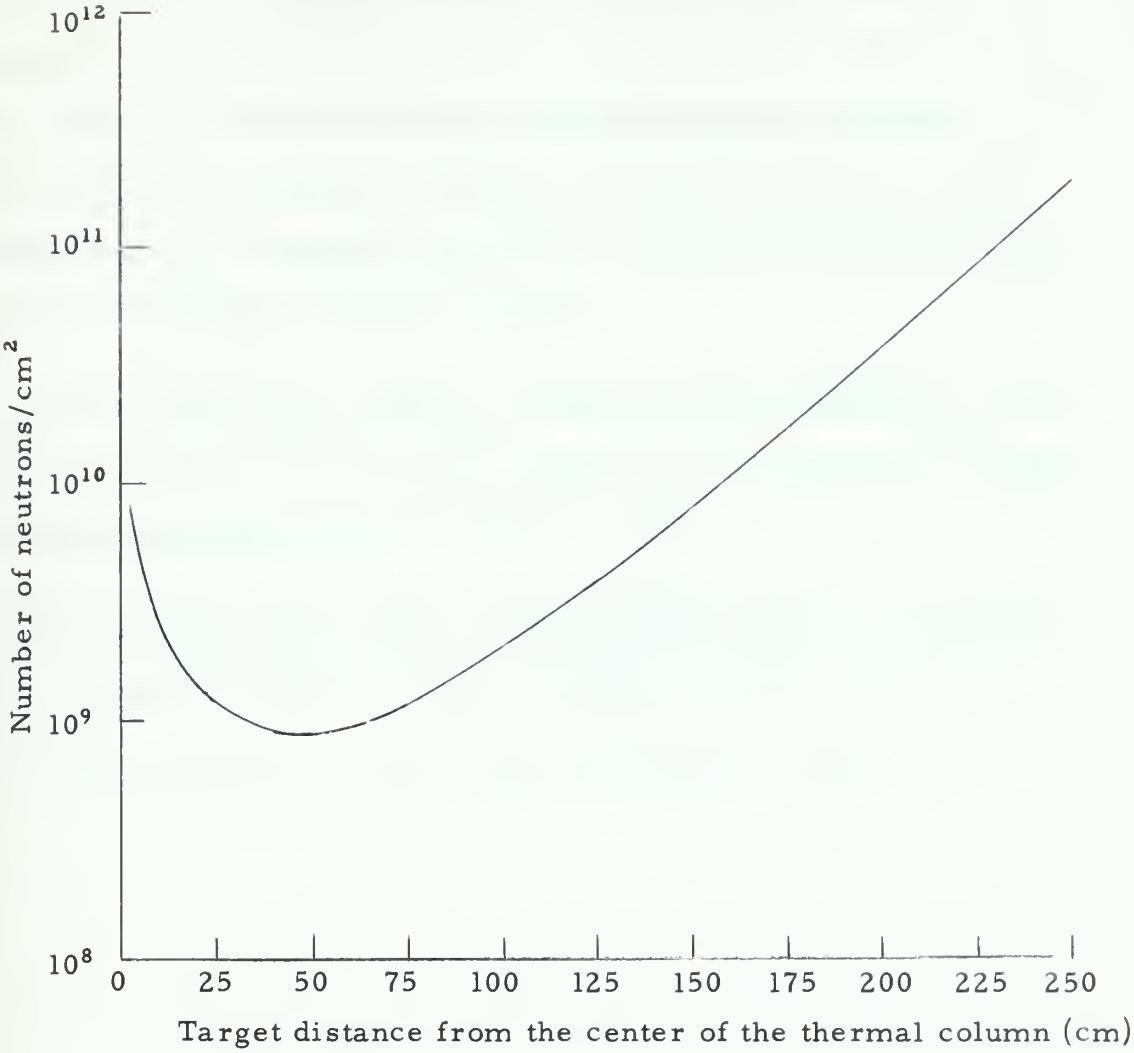

Fig. 6 The number of neutrons-cm^2 passing through a target during the maximum exposure time as a function of the distance of the target from the center of the thermal column face.

Optimum exposure times and distances

The maximum permissible gamma ray dose rate that a recording emulsion was to be allowed to receive was set at that received by an emulsion exposed for 5 minutes at the center of the thermal column face behind 2" of lead shielding and with the reactor operating at 100 kw. This choice of the maximum permissible dose was based on Sattler[2] having found that exposure under these conditions was about the upper limit for obtaining a readable emulsion.

Figure 5 shows the maximum exposure time consistant with the maximum gamma ray dose rate as a function of the distance in water between the emulsion and the thermal column.

Figure 6 shows the number of neutrons per square centimeter expected to pass through the target at maximum exposure time as a function of the target's distance from the thermal column.

III. EQUIPMENT AND EXPERIMENTAL PROCEDURE

Equipment

Consideration of the factors discussed in the preceding chapter on "Theoretical Background", the availability of materials, and the desirability of keeping the recording emulsion out of the neutron beam and positioned in such geometry as to prevent large dip angles for particles entering the emulsion led to the design of a nuclear emulsion exposure chamber as shown in the cutaway sketch of Figure 7.

The chamber has the following features not immediately obvious from a glance at the sketch:

(a) The target plate and the recording emulsion holders are adjustable with respect to position on the support rod and in angle of inclination.

(b) The vacuum connection is a 3/4" O. D., 3/8" I. D. tube which is connected to a standard 5/8" I. D., 3/8" wall thickness, rubber vacuum hose.

(c) The chamber bottom plate is fitted with a standard 1/8" "O" ring.

(d) All components of the chamber including the nuts and bolts are of 2S aluminum alloy. The shortest half life of radioactivity induced by the exposure of aluminum to thermal neutrons is obtained by using a 2S aluminum alloy (half life 2.5 minutes). Therefore, the use of this alloy insured that the time between exposure of the nuclear emulsions at the reactor and their unloading from the chamber in a photographic darkroom would not be excessive due to having to wait long periods

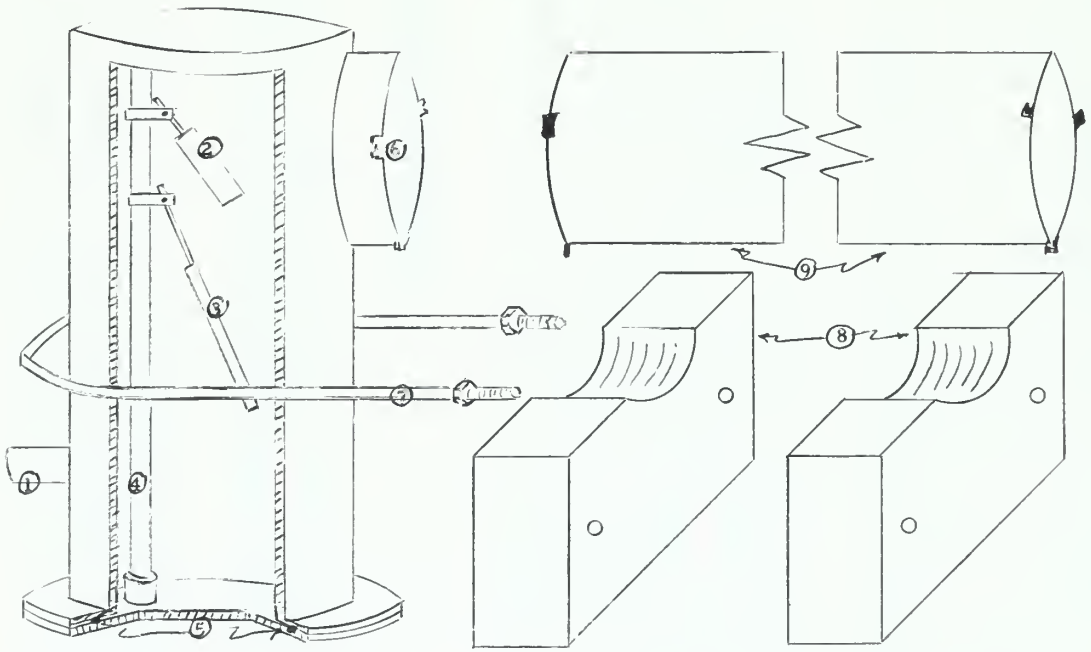

LEGEND

1 Vacuum connection
2 Target plate holder
3 Nuclear emulsion holder
4 "O" ring vacuum seal
5 Support rod
6 Incident beam tube connection
7 Lead brick clamp
8 Lead shielding bricks
9 Incident beam tubes (3 tubes of length 1', 3', and 4').

Fig. 7 Cutaway sketch of the nuclear emulsion exposure chamber assembly.

of time after exposure for the activity of the chamber to die out to the extent that handling became safe.

(e) The eight feet of incident beam tube is sectioned in lengths of one, three, and four feet to permit a variation in beam length. Each end of the tubes is sealed with welded face plates and fitted with lugs for attachment in one continuous tube or individually to the beam tube connection on the chamber. The tubes are water tight and air filled.

Auxiliary equipment used in this investigation consisted of a J. M. Welch Duo-Seal vacuum pump, 30 feet of 3/8" I. D. vacuum hose, a standard 0-760 mm of mercury vacuum guage, standard photographic darkroom equipment, and a Lietz Ortholux microscope.

As the investigation progressed, it was necessary to provide for complete lead shielding of the nuclear emulsions during exposure. The lead shielding insert for the exposure chamber is illustrated in Figure 7 (a). Figure 7 (b) is an illustration of a cadmium liner for the lead shield which was deemed necessary at one point in the investigation.

Fabrication of target plates

A number of targets were made for use in this investigation, much of the detail in their fabrication is listed in Table 2.

There were two basic methods used in making the targets. The first method consisted of spraying the target material on the back-up plate with an ordinary atomizer. After spraying, the back-up plate

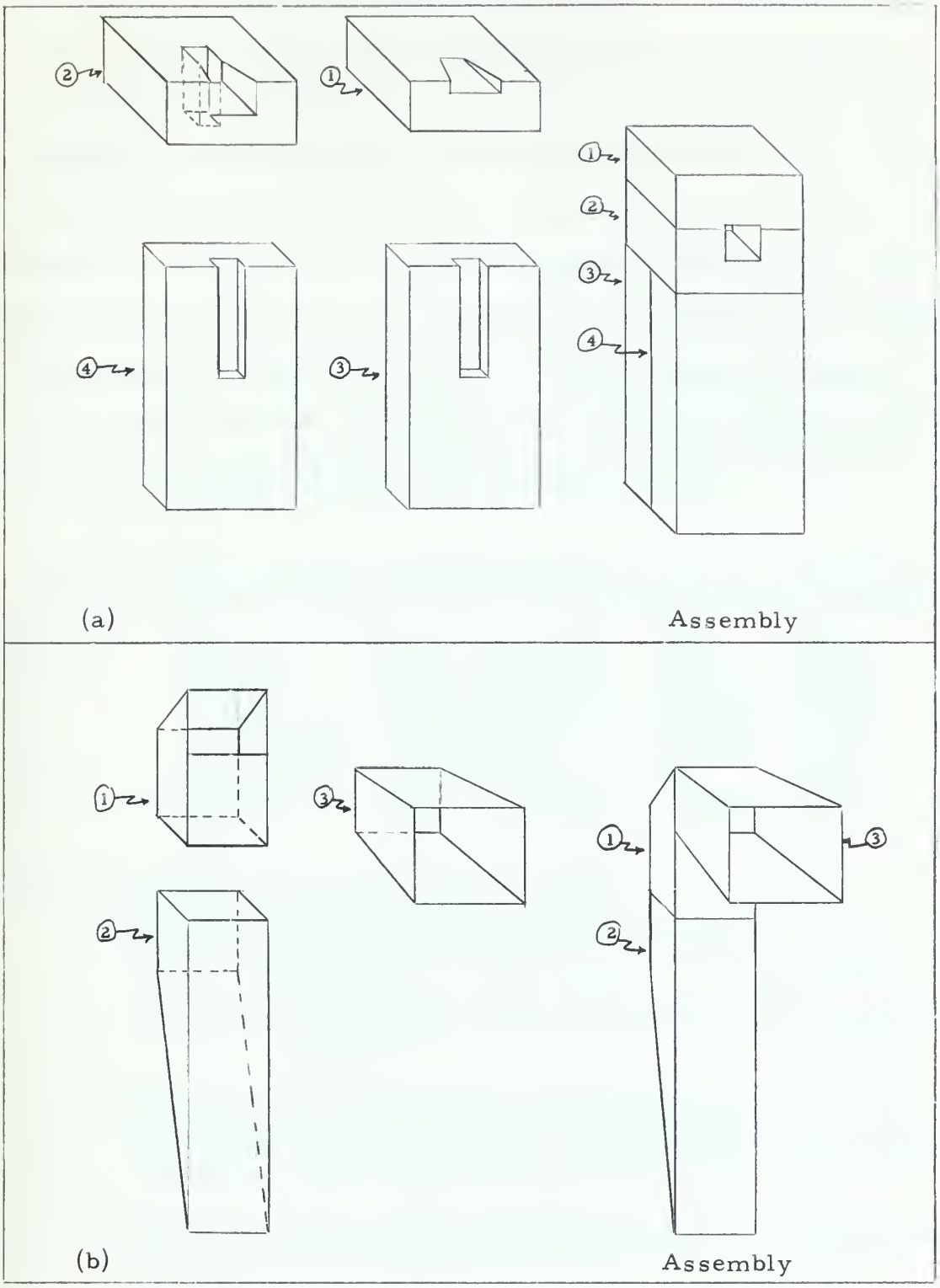

Fig. 8. (a) Lead shield insert for nuclear emulsion exposure chamber.
(b) Cadmium liner for lead shield.

was placed on a lukewarm hotplate and the water was allowed to evaporate prior to the next spraying operation. In the second method, a predetermined amount of solution was poured into a pan made of the target back-up plate material and the water was allowed to evaporate at room temperature. This left the target material deposited over the large surface of the pan and the back-up plate was then cut out of the pan. Evaporation of the target material on to the target back-up plate was necessary in order to get plates of the thin film type required (.141 mg/cm^2). Of the two methods used, the second seemed to give the more homogenous distribution of target material.

Table 2. Characteristics of target plates used in the investigation

(1)	(2)	(3)	(4)	(5)
1	4x4 cm	.0005" aluminum	.0143	.0286
2	4x4 cm	.0005" aluminum	.000304	.0255
3	2.5x2.8 cm	.005" aluminum	.000304	.0255
4	2.5x2.8 cm	.05" cadmium	.000304	.0255
5	2.5x2.8 cm	.005" aluminum	0	0
6	4x4 cm	.0005" aluminum	.000304	.0255
7	4x4 cm	.0005" aluminum	0	0

Note: (a) Column 1 is the target plate number.
Column 2 is the target plate size.
Column 3 is the material used and its thickness.
Column 4 is the surface density of lithium in the target (mg/cm^2)
Column 5 is the surface density of nitrogen in the target in (mg/cm^2)

(b) Plates 1 and 2 were made by spraying solution on with an atomizer and evaporating over a hotplate. All other plates were made by allowing solution to evaporate at room temperature in a pan made of target back-up material.

(c) Plates 5 and 7 were not coated with target material and were used in the determination of background track counts.

Description of nuclear emulsions used

The nuclear emulsions used in this investigation were of three types; Ilford K2 emulsions, Ilford C2 emulsions, and Kodak NTA emulsions.

The Ilford K2 emulsions were 50 microns thick and were mounted on 1"x3" glass plates. They are sensitive to protons up to about 80 Mev and to tritons and alpha particles of correspondingly higher energies. The K2 plates replace the C2 plates that were once manufactured by Ilford and are quite similar in characteristics to the C2 plates. The protons, alpha particles, and tritons encountered in this investigation were expected to produce tracks of the following lengths in the emulsion[13].

Particle	Energy	Range in emulsion
Proton	.584	6.7 μ
Alpha	2.052	6.7 μ
Triton	2.736	34 μ

The Ilford C2 emulsion, as mentioned previously, is similar in characteristics to the K2 emulsion. The notable difference as elicited in this investigation is that the C2 emulsions seem to be more sensitive to gamma radiation than the K2 and, consequently, give a decidedly darker plate when exposed to the same gamma ray dose rate as the K2. The plates used in this investigation were 50 microns thick and were mounted on 1"x2" glass plates.

The Kodak emulsions used were NTA 25 micron plates on a 1"x3" glass backing. The NTA emulsions are sensitive to protons up to an energy of 3 Mev and are sensitive to alpha particles and tritons of correspondingly higher values. The range of the various particles is expected to be about the same as for the Ilford emulsions.

Experimental geometry

The diameter of the incident beam of thermal neutrons was 3.5" and the length of the beam from the face of the thermal column to the center of the target plate was one of three values (10 cm, 40 cm, or 100 cm) for the various exposures used in the experiment.

The centers of the target plate and the recording emulsion were either 10 cm or 12.5 cm apart, depending on the exposure. The target plate was inclined to the normal of the chamber at 45^0 and the emulsion was inclined at 15^0 as is illustrated in Figure 9.

The position of the emulsion with respect to the target insured:

(a) that the maximum angle of dip that a track coming from the target could make in the emulsion was 40^0 and the minimum 10^0,

(b) that all particles entering the emulsion from the target would be within 30^0 of a line from the top to the bottom of the emulsion and parallel to a side of the emulsion, and

(c) that no part of the emulsion lay in the direct neutron beam.

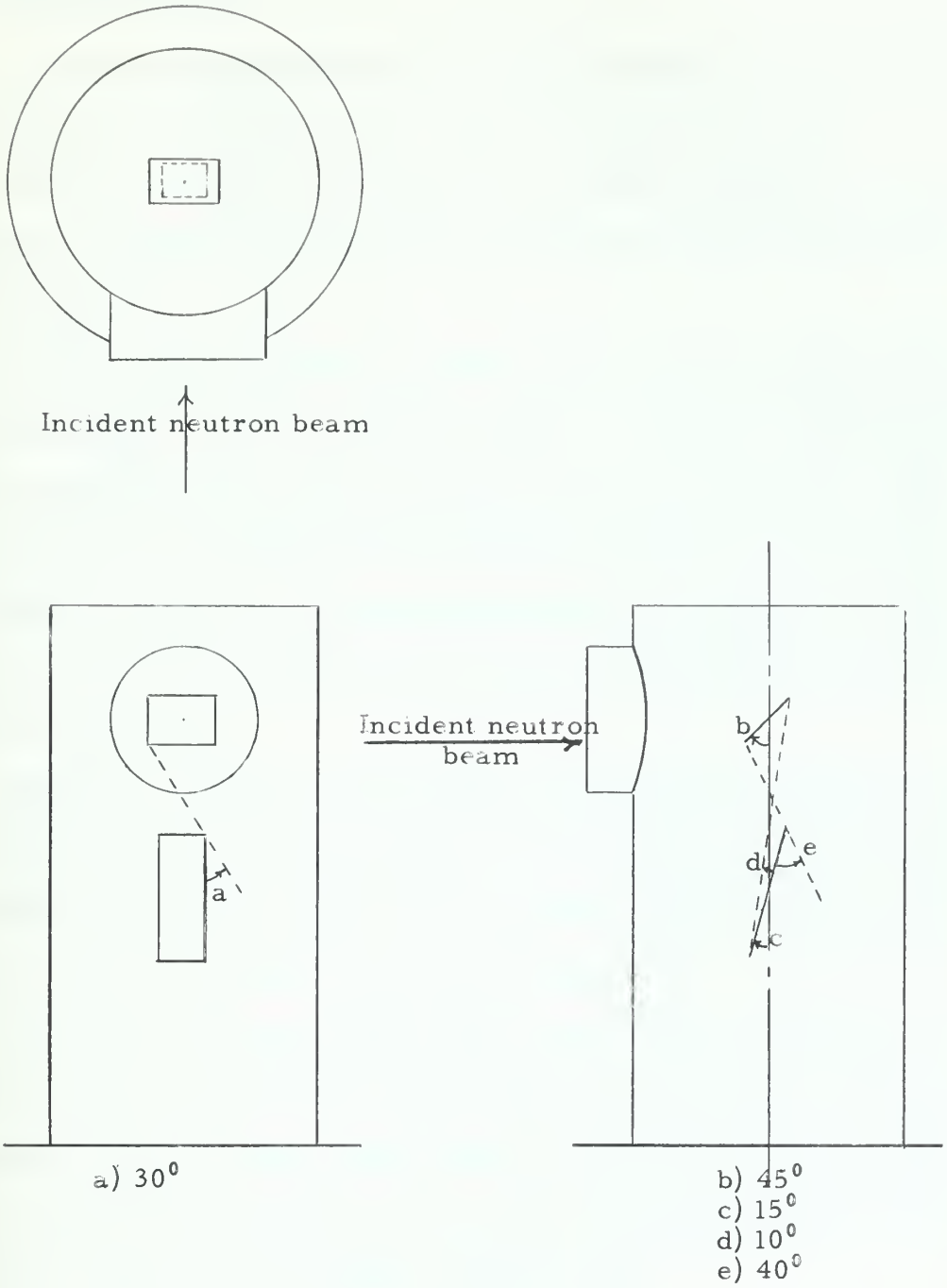

Fig. 9. System geometry for exposure of nuclear emulsions.

Exposure of the nuclear emulsions at The Pennsylvania State University Research Reactor

The following procedure was used in the exposure of all nuclear emulsions worked with in the course of this investigation.

(a) The emulsion to be exposed was loaded into position in the exposure chamber in a photographic darkroom using a Wratten Series 1 safelight.

(b) The loaded chamber was taken to the reactor facility where the lead bricks, which were used to weight the chamber down and aid in the reduction of the gamma ray dose rate at the emulsion, were strapped to the chamber. The vacuum pump was connected to the chamber via 30 feet of vacuum hose and the pump run for about 10 minutes prior to the lowering of the chamber into exposure position in the reactor pool.

(c) The appropriate incident beam tube extension was bolted to the chamber and the entire assembly was lowered into exposure position behind the thermal column. The arrangement used in the exposure of the nuclear emulsions is pictured in Figure 10.

(d) With the vacuum pump running continuously to maintain a vacuum of at least a hundredth of an atmosphere in the chamber during the exposure and with guy ropes holding the chamber steady in position, the target was irradiated with a thermal neutron flux at full reactor power (200 kw) for the proper exposure time.

(e) Upon completion of exposure, the entire assembly was brought to the surface of the pool where it was monitored for radioactivity. The front of the beam tube extension normally read well over one

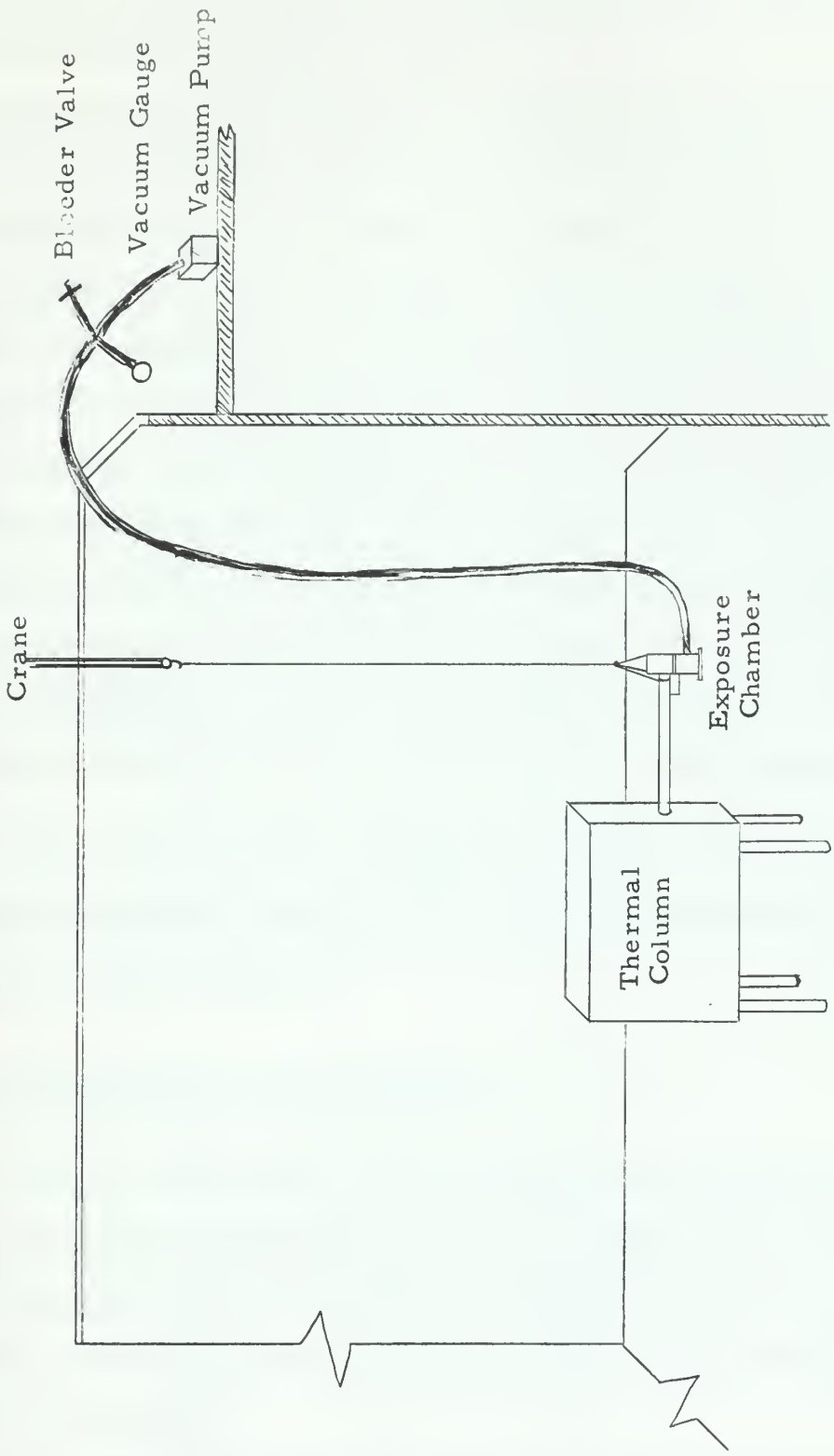

Fig. 10. Equipment arrangement during exposure of nuclear emulsions.

roentgen per hour while the main body of the chamber itself read only about forty milliroentgens per hour.

(f) The beam tube extension was removed from the chamber and stored underwater until it had decayed in activity sufficiently to permit safe handling. The chamber was removed from the pool, the lead unstrapped, the vacuum eased off the chamber by opening the bleeder valve to the atmosphere, and the vacuum pump was disconnected. After these steps had been completed, the activity of the chamber had decreased to a value sufficiently low to make it safe for the chamber to be moved from the reactor facility (usually about 15 minutes).

(g) The chamber was taken to a darkroom and was unloaded. The emulsion was then developed and processed as soon as it was practicable so as to prevent latent image fading in the emulsion which might be caused by too long a delay between exposure and processing.

Table 3 lists the exposures that were made pursuant to this investigation together with pertinent remarks concerning the special features of each exposure.

Processing of the nuclear emulsions

Since all of the nuclear emulsions processed were 50 microns or less in thickness, none of the special precautions or procedures that must be observed in the handling of the thicker emulsions were necessary and the processing procedure followed was that which is recommended by Beiser[14].

(a) The plates were developed in Kodak D-19 developer for 3.5

Table 3. Data on exposures made during $N^{14}(n, p)C^{14}$ cross-section investigation

Exposure No.	Exposure distance	Exposure time	Emulsion type	Target No.	Shielding
1	100 cm	90 min	K2 50μ	1	4" lead
2	100 cm	90 min	NTA 25μ	2	6" lead
3	100 cm	90 min	K2 50μ	2	do
4	100 cm	90 min	K2 50μ	3	lead insert
5	100 cm	180 min	K2 50μ	3	do
6	100 cm	270 min	K2 50μ	3	do
7	40 cm	60 min	K2 50μ	4	lead insert cad. liner
8	10 cm	3 min 36 sec	K2 50μ	4	do
9	100 cm	270 min	K2 50μ	4	do
10A	100 cm	270 min	NTA 25μ	3	do
10B	100 cm	270 min	NTA 25μ	3	do
11	100 cm	160 min	NTA 25μ	3	all lead and cadmium removed from back of target
12	100 cm	270 min	NTA 25μ	3	no cadmium
13	100 cm	270 min	NTA	3	all lead in direct neutron beam removed
14	100 cm	270 min	K2 50μ	3	do
15	100 cm	270 min	K2 50μ	5	do
16	100 cm	90 min	C2 50μ	6	same as 1
17	100 cm	90 min	C2 50μ	7	do

minutes at 20^0 C and with no agitation.

(b) The plates were placed in a one percent solution of acetic acid stop bath at 20^0 C for a period of 10 minutes with slight agitation. While in the stop bath, the plates were rubbed lightly with the finger tips to remove suface deposits.

(c) The plates were then fixed in Kodak F-5 fixing bath for a period of about 30 minutes (one and one half the time it took for the plates to clear) at 20^0 C. Agitation in the fixer was continuous and was done with a wide swath stirring rod by hand.

(d) After fixing, the plates were washed in running water for about 30 minutes prior to drying at room temperature in a humid atmosphere.

Microscope technique used in reading nuclear emulsions

The plates were initially scanned using 25x periplanatic eyepieces with 100:1 oil immersion objectives in a Lietz Ortholux microscope. This combination of eyepiece and objective gave an over-all magnification of 3200 in a field of view of 5.03×10^3 microns^2. Because of the very few tracks seen per field of view at this magnification and for greater ease in seeing the tracks against the fairly heavy fog background encountered, the magnification was reduced to 660 by using 10x eyepieces and a 53:1 oil immersion objective. With the magnification at 660, the effective area of the field of view was increased to 5.95×10^4 microns.^{2}

The best contrast between the tracks and the fog background consistant with an illumination that would not cause excessive eyestrain

after long periods of viewing was obtained with a green filter in the lamp housing and a setting of 4 on the Regel-Transformator.

According to the literature,[14,15,16,17] one should be able to distinguish between proton tracks and alpha particle tracks of the same length in a nuclear emulsion due to the difference in their respective ionization abilities. However, during this investigation, it was not possible to make this distinction with any degree of assurance that proton tracks were not being counted as alpha particle tracks or vice versa. The inability to make a distinction between the alpha particles and the protons was probably due to the shortness of the tracks involved (less than 6.7 microns). As a result, the best that could be done was to count short tracks (6 micron alpha particles and protons) and long tracks (34 micron tritons).

The first 100 tracks counted were measured in length in order to get a feeling for the identification of the alpha particle, proton, and triton tracks. The short tracks varied in length from 4.5 to 6.5 microns and the long tracks varied from 29 to 34 microns in length.

In counting tracks, only those tracks whose geometry was consistant with that of the experimental setup were counted. If a track was inclined to the horizontal at an angle greater than 30^0, did not appear to enter the emulsion from the surface, dipped at an angle greater than 40^0, or entered the emulsion in the wrong direction then it was not counted. Figure 11 illustrates the criteria used for determining whether or not a track was to be counted.

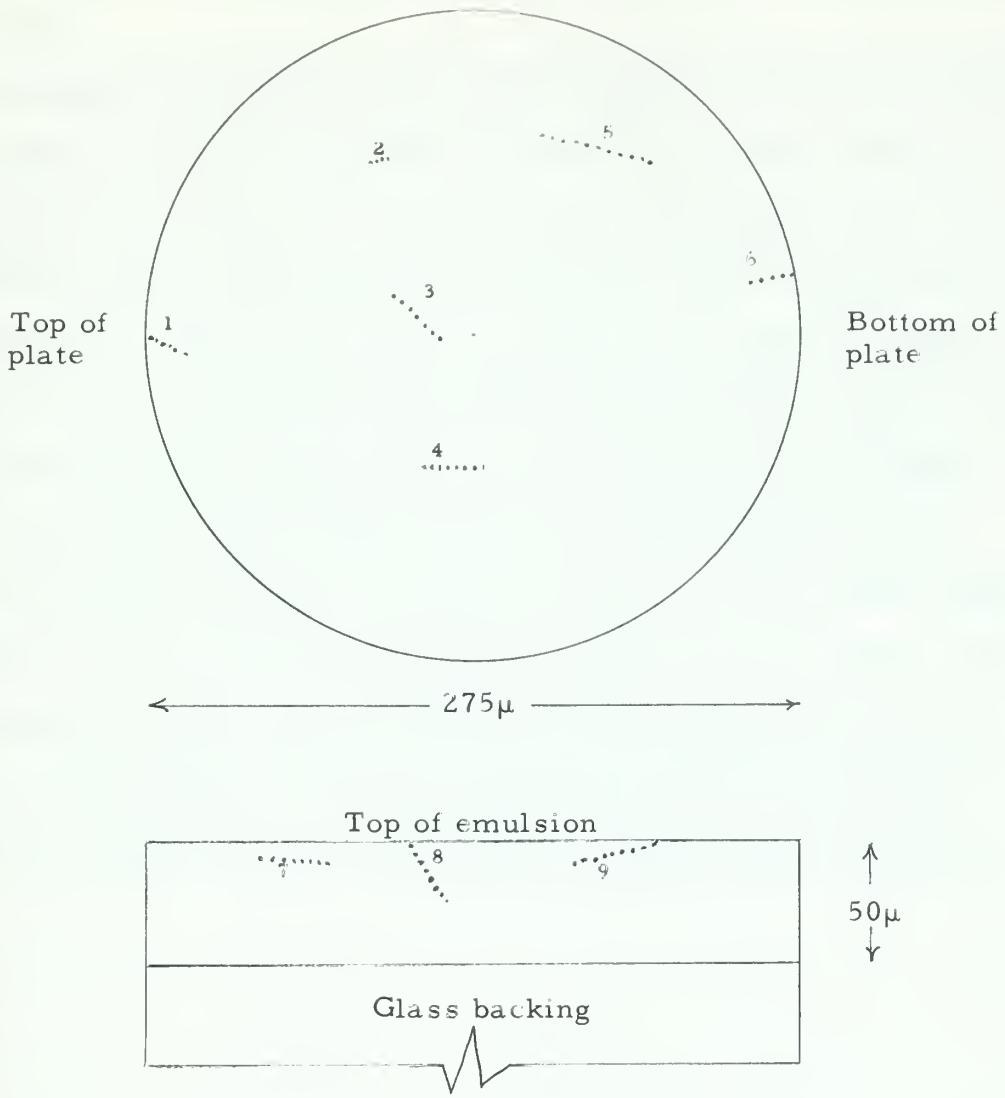

1 Not countable - Track starts out side of field of view
2 Not countable - Track shorter than 5μ
3 Not countable - Track makes an angle greater than 30^0
4 Not countable - Track less than 27 and greater than 6.5μ
5 Not countable - Track longer than 34 μ
6 Countable - Track begins in the field of view
7 Not countable - Track begins in the emulsion vice surface
8 Not countable - Track dips at an angle greater than 40^0
9 Not countable - Track starts at bottom of plate traveling toward the top

Fig. 11. Sketch of a microscope field of view illustrating the criteria used in counting tracks.

The following procedure was used in scanning the plates and counting tracks:

(a) The first field of view was taken at a position which lay 1/4" from the right end of the plate and 1/8" in from the lower edge of the plate.

(b) Successive fields of view were taken by shifting the plate down a distance equal to the diameter of the field of view. At the top of the plate the microscope stage was then shifted over a distance equal to the diameter of the field of view and the same procedure was followed to the bottom of the plate, and so on to the completion of counting.

(c) The short tracks of each field of view were counted first by slowly moving the surface of the plate in and out of focus while noting whether the short tracks being viewed originated at the surface or not. The same procedure was then applied to the counting of long tracks. Tracks which appeared doubtful in their geometry or length were measured with the eyepiece graduated scale and compass reticule.

IV. EXPERIMENTAL RESULTS

Preliminary results of individual exposures

The experimental arrangement for each successive exposure was designed to improve upon the readability of the preceding plate so that the experiment might culminate in an exposure which could permit an accurate determination of the $N^{14}(n, p)C^{14}$ thermal neutron cross-section. Therefore, the most orderly presentation of the results of this investigation is given by considering the various plates in the sequence in which they were exposed.

Plate 1

This plate was an Ilford K2, 50 micron, 1"x3" nuclear emulsion exposed with the target at a distance of 100 cm from the face of the thermal column and with an exposure time of 90 minutes. The plate was shielded with 4" of lead between the plate and the thermal column.

The plate was scanned with a Lietz Ortholux microscope using 25x periplanatic eyepieces and a 100:1 oil immersion objective. Although the fogging due to the gamma radiation received by the emulsion during exposure was moderate, the tracks could be seen clearly and 300 fields of view were taken. There were 36 tracks counted in the 300 fields of view, 19 of the tracks were short and 17 were long. In this plate, as well as in all others subsequently scanned, it was not possible to differentiate between the 6 micron proton tracks and the 6 micron alpha particle tracks. As a result, the statistics of the experiment

were destined to be quite poor unless the ratio of the nitrogen to the lithium contained in the target was greatly increased. This facet of the investigation will be discussed in more detail in the discussion of errors later in this chapter.

Although plate 1 was readable, the fogging was at about the upper limit of acceptability and any further fogging would have rendered the short tracks quite difficult to see and count.

Plates 2 and 3

The exposure of these two plates was identical to that of plate 1 with the following variations:

(a) An additional 2" of lead was placed between the plates and the thermal column giving a total of 6" of lead shielding. This was done to determine the effect on the fogging of the plates when additional lead was placed between them and the thermal column.

(b) A new target was used which contained a mixture of $LiNO_3$ and $NaNO_3$ in amounts such that the ratio of the surface density of lithium to the surface density of nitrogen was .0119. This has the effect of causing one alpha particle track and one triton track to be seen in the emulsion for each proton track seen. All subsequent exposures (except those made for background determinations) were made with targets using this same ratio of lithium to nitrogen.

(c) Two plates were exposed simultaneously, one being a Kodak NTA emulsion (plate 2) and the other an Ilford K2 (plate 3). The purpose of the two plate exposure was to compare the fogging in these two differ-

ent type emulsions when exposed under identical conditions.

The Kodak NTA, 25 micron, 1"x3" nuclear emulsion was decidedly darker due to gamma blackening than the Ilford K2. It was fogged to such an extent that all tracks were lost in the fog grain background and no scanning of this plate was accomplished beyond that necessary to determine its condition.

The Ilford plate was similar in fog grain density to that of plate 1, indicating that the addition of the 2" of lead had little or no effect. This was taken to mean that the source of gamma radiation was the capture gamma rays of water in the area of the chamber or the gamma rays of neutron absorption by the chamber aluminum.

Using the same magnification as was used on plate 1 (3200), plate 3 was scanned for 500 fields of view. In the scanning 4 short tracks were counted and no long tracks. The plate was then scanned by moving the plate slowly past the objective for several lengths of the plate. A few long tracks were found by this method of scanning which indicated that the exposure and processing had not been faulty but that the time of exposure had been insufficient to produce an effective number of tracks per field of view.

Plates 4, 5, and 6

The source of the gamma blackening having been determined as the capture gamma rays of the water in the vicinity of the chamber or the neutron absorption gamma rays of the chamber aluminum, a lead

shield was built which provided the needed protection from gamma rays coming in any direction and which was of such a size as to be able to be inserted into the chamber itself. Figure 8 is an illustration of this shielding.

Plates 4, 5 and 6 were all Ilford K2 emulsions and were exposed in succession without waiting to scan the one before exposure of the next. This was done to take advantage of reactor time available during this stage of the investigation. The plates were exposed at a distance of 100 cm from the thermal column for periods of 90, 180, and 270 minutes respectively. The 4" of lead in front of the plates was supplemented by the interior lead shielding of the chamber. This shielding arrangement gave a minimum of 2" of lead in all directions.

The fog grain background of the plates varied as the time of exposure, however, all plates had less background than either plate 1 or plate 3. It was felt that the time of exposure could be lengthened to about 7 or 8 hours without passing the acceptable background limit.

Plate 4 was scanned using a magnification of 3200 for 300 fields of view. During the scanning, 67 short tracks were counted and 2 long tracks. Since the expected ratio of the number of short tracks to the number of long tracks was 2 to 1, the observed ratio of 33.5 to 1 indicated that the addition of the lead to the interior of the chamber had introduced a large source of background tracks. Scanning the emulsion from top to bottom showed that a large number of short tracks were to be found originating in the emulsion itself. These tracks were

thought to be proton tracks from $N^{14}(n, p)C^{14}$ reactions caused by the scattering of thermal neutrons from the incident beam by the lead shielding in the interior of the chamber.

A scanning of plates 5 and 6 yielded results similar to those of plate 4 except for a larger number of tracks per field of view due to the greater time exposure of these plates.

Plates 7 and 8

To reduce the number of background tracks encountered in plates 4, 5, and 6, a cadmium liner for the interior lead shielding was designed and fabricated as illustrated in Figure 8 (b). The purpose of the cadmium liner was to absorb those neutrons which might otherwise scatter off the lead and enter the nuclear emulsion to cause n-p reactions in the nitrogen atoms of the emulsion.

Plate 7 was an Ilford K2 emulsion exposed for 60 minutes with the target at a distance of 40 cm from the face of the thermal column. The emulsion was shielded from the capture gamma rays in water and the aluminum gamma rays by the lead interior shielding and was shielded from the thermal neutrons by a cadmium liner in the lead.

Plate 8 was exposed under the same experimental setup as plate 7 except that the exposure distance and the time were shortened to 10 cm and 3 minutes 36 seconds respectively.

Neither plate produced tracks that were visible through the extremely heavy gamma radiation fogging that resulted at the new

exposure times and distances. No further exposures were made at these distances. All subsequent plates were exposed at a distance of 100 cm from the face of the thermal column.

Plate 9

Plate 9 was an Ilford K2 and was exposed with the same shielding as was used for plates 7 and 8. The plate was exposed with the target, once again, at 100 cm distant from the thermal column and with an exposure time of 270 minutes.

Plate 9 was placed in the developer for a period of only 2 minutes instead of the 3.5 minutes of developer time given to all other plates. This was done to determine if the shorter development time would increase the contrast between the fog grain background and the charged particle tracks. If so, then longer exposures could be made with an attendant increase in the number of tracks per field of view. Apparently the development time was too short since no tracks were seen in the considerable area scanned. The normal stars that can be seen originating in unexposed emulsions were barely visible.

At this point in the investigation, there were only two Ilford K2 nuclear emulsion plates left. Therefore, it was decided to make all subsequent exposures with the Kodak NTA emulsions until an optimum exposure arrangement was reached, at which time, the two Ilford K2 plates would be exposed, one for track counting and the other for the background track determination.

Plates 10A and 10B

Both of these plates were Kodak NTA, 25 micron, 1"x3" nuclear emulsions and were exposed with the same shielding used in the exposure of plates 7, 8, and 9. The target was placed 100 cm from the thermal column and the plates exposed for 270 minutes. Plate 10A was placed in the normal exposure position in the chamber and Plate 10B was positioned so as to be normal to the incident neutron beam and outside of the cadmium liner as is illustrated in Figure 12. This arrangement was designed to determine whether the thermal neutrons which had entered the emulsions of plates 4, 5, and 6 came predominantly from the top and back of the chamber, the front of the chamber, or equally from all directions. It was proposed to make this determination by comparing the number of tracks per unit volume in plate 10B with that in plate 6. If the number in 10B were equal to one third the number in plate 6, then the distribution would be isotropic. If it were less than one third the number in 6, then most neutrons came from the top and back . If the number is greater than one third the number in 6, then most came from the front of the lead shielding insert.

Both plates were too fogged by gamma radiation to permit the viewing of any tracks. The gamma blackening was decidedly heavier at the top of the plates than at the bottom. This variation in intensity from heavy at the top to lighter at the bottom of the plates seems to indicate that the gamma radiation seen was a capture gamma ray of one of the cadmium isotopes or, possibly, not gamma radiation at all

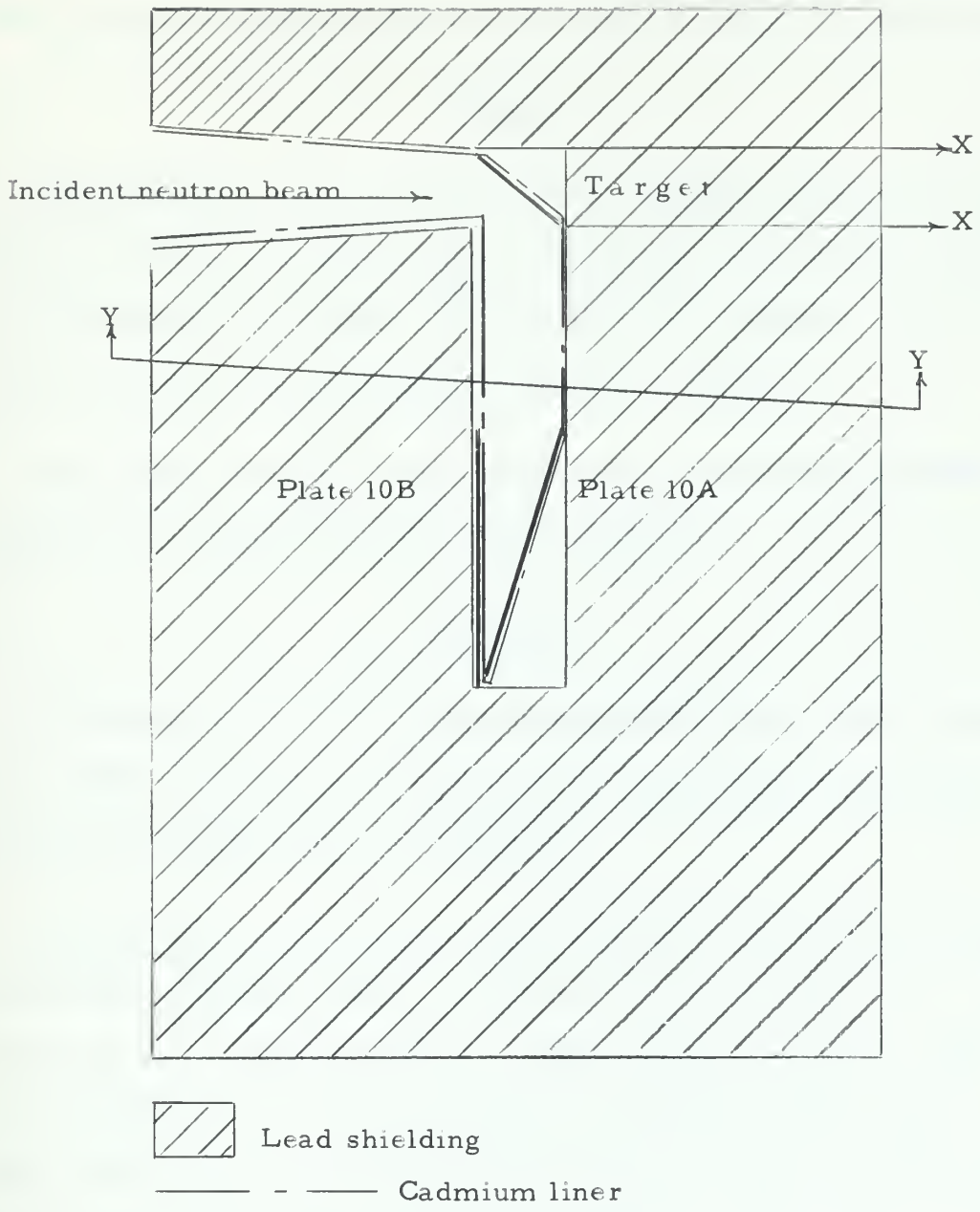

Fig. 11. Sketch illustrating (a) plate arrangement for exposure 10 (b) section XX - lead shielding removed for exposures 11 12, and (c) section YY - lead shielding removed for exposures 13, 14, and 15.

but the .58 Mev beta particles of Cd^{113} decay. At any rate, the blackening resulted from that cadmium which was in the direct neutron beam.

Plate 11

This Kodak plate was exposed with the cadmium and the lead which had been directly behind the target removed (see section XX in Figure 12). The exposure was made at 100 cm but with an exposure time of only 160 minutes due to an unexpected reactor shutdown.

Once again, the plate was too blackened to be read and another exposure was made after removing all cadmium.

Plate 12

The exposure of this plate was identical with that of plate 6 except that a Kodak NTA was used instead of the Ilford K2 and the lead directly in back of the target had been removed.

Although there were tracks visible through the gamma background, an accurate counting of tracks on this plate was not possible due to the density of the background making it highly probable that many short tracks would be missed in the counting. A scanning of the plate in depth revealed that many background tracks were still present despite the removal of the lead in back of the target.

Plate 13

For this exposure all lead in the direct neutron beam was removed as indicated in Figure 12, section YY. The exposure distance and time

were, again, 100 cm and 270 minutes.

This plate was the best of the Kodak NTA's exposed but due to the density of the background was still not countable with any degree of accuracy. However, it was felt that the Ilford K2's exposed under the same conditions would yield satisfactory plates and it was decided that the last two Ilford K2's could now be used for a final set of exposures.

Plates 14 and 15

These plates were Ilford K2, 50 micron nuclear emulsions and were exposed with the target at a distance of 100 cm from the face of the thermal column for a period of 270 minutes. There were 4" of lead shielding between the chamber and the thermal column in addition to a partial lead shield in the exposure chamber itself.

Plate 14 was exposed with a normal $LiNO_3$-$NaNO_3$ target. Plate 15, which was to be used to count background tracks, was exposed using only a target of aluminum foil similar to that on which the target material was deposited on.

The removal of all lead in the direct neutron beam left the emulsions unshielded to the capture gamma rays of the water directly over the chamber. This caused excessive darkening of the plates and they were unable to be used for the determination of the $N^{14}(n, p)C^{14}$ cross-section.

Plates 16 and 17

All the available Ilford K2 plates having been used, two last exposures were made using some Ilford C2, 50 micron, 1"x2" nuclear emulsions. They were exposed under identical conditions to those used in the exposure of plate 1 except for the target being one with a $LiNO_3$-$NaNO_3$ mixture vice the $LiNO_3$ alone of plate 1. Plate 1 had been an entirely satisfactory plate except for the poor statistics that resulted from not being able to differentiate between the alpha particle and proton tracks.

Although the C2 plates are said to be quite similar in characteristics to the K2 plates which replaced them in the Ilford line,[18] they are apparently more sensitive to the gamma radiation encountered in this investigation for exposure under the same conditions rendered the C2 plates unreadable where the K2 plates had been satisfactory.

Final results of the investigation of the thermal neutron cross-section of the $N^{14}(n, p)C^{14}$ reaction

Despite the extremely poor statistics involved in the use of plate 1 in a determination of the $N^{14}(n, p)C^{14}$ cross-section, plate 1 was counted and used for this purpose since of the 17 plates exposed, it was the only plate which was not made unusable by either excessive gamma blackening, excessive background tracks, or too few tracks per field of view

An unexposed plate and plate 3 were used in conjunction with plate 1 in order to get a reasonable estimate of the number of background

tracks included in the total track count of plate 1. Plate 3 had been exposed under the same conditons as used for the exposure of plate 1 with the exception that the ratio of the lithium surface density in plate 3 to that in plate 1 was 47 and the ratio of the nitrogen surface densities was 1.122.

Scanning of the plates for the final determination of the cross-section was done on a Lietz Ortholux microscope using 10x periplanatic eyepieces with 53:1 oil immersion objective. This combination of eyepiece and objective resulted in a magnification of 660 and a field of view with area 5.9×10^4 microns^2.

A total of 4967 fields of view were counted on plate 1. There were 3452 long tracks and 3627 short tracks (695 long and 730 short tracks per 1000 fields of view). Plate 3 gave 49 long tracks and 67 short tracks in the 1000 fields of view taken of it. The unexposed plate had 19 long tracks and 22 short ones in 1000 fields of view.

The poor statistics and the unavailability of a true background count for plate 1 resulted in the inability of the investigator to obtain the cross-section of the $N^{14}(n, p)C^{14}$ reaction to a better degree of accuracy than the setting of an upper limit to the value possible. The results of this investigation show the value of the cross-section to be less than 5 ± 1 barns. The result was arrived at as indicated in the derivation given in the next paragraph.

In the following derivation, all numbers will be based on 1000 fields of view.

Let N_l^i be the total number of long tracks counted on plate i

N_s^i be the total number of short tracks counted on plate i

N_p^i be the number of proton tracks on plate i

N_a^i be the number of alpha particle tracks on plate i

N_t^i be the number of triton tracks on plate i

N_{lb}^u be the number of long background tracks counted on the unexposed plate

N_{sb}^u be the number of short background tracks counted on the unexposed plate

N_{lb}^i be the number of long background tracks on plate i less N_{lb}^u

N_{sb}^i be the number of short background tracks on plate i less N_{sb}^u

R be the ratio of the surface density of lithium on plate 3 to that on plate 1

Since plates 1 and 3 were exposed under the same conditions, it is reasonable to assume that their backgrounds will be the same. This assumption will be used in the derivation given below.

$$N_t^i + N_{lb}^i + N_{lb}^u = N_l^i \ ;$$

therefore, $N_t^1 + N_{lb}^1 = N_l^1 - N_{lb}^u$

and $N_t^3 + N_{lb}^3 = N_l^3 - N_{lb}^u$.

Since $N_{lb}^1 = N_{lb}^3$

and $N_t^3 = 1/R \ N_t^1$,

then $1/R \ N_t^1 + N_{lb}^1 = N_l^3 - N_{lb}^u$

and $N_t^1 + N_{lb}^1 = N_l^1 - N_{lb}^u$

Solving the last two equations simultaneously, we have

$$N_t^1 = R/(R-1)\ (N_1^1 - N_1^3) = N_a^1 = 47/46\ (695 - 49) = 660$$

We solve now for the number of proton tracks plus the background tracks due to exposure of plate 1.

$$N_p^1 + N_a^1 + N_{sb}^i + N_{sb}^u = N_s^i\ ;$$

therefore, $N_p^1 + N_{sb}^1 = N_s^1 - N_{sb}^u - N_a^1 = N_s^i - N_{sb}^u - R/(R-1) \cdot (N_1^1 - N_1^3)$

$$= 730 - 22 - 660 = 48$$

Note that equation (4) in chapter 2 reads:

$$\sigma_{N^{14}} = \frac{N_p}{N_t} \frac{I_{Li^6}}{I_{N^{14}}} \sigma_{Li^6}$$

Therefore, $\sigma_{N^{14}} < \frac{N_p + N_{sb}}{N_t} \frac{I_{Li^6}}{I_{N^{14}}} \sigma_{Li^6}$.

Substituting the appropriate numbers in the above inequality, we have the result that

$$\sigma_{N^{14}} < \frac{48 \times .0742 \times 945}{660 \times .996337} \doteq 5 \text{ barns.}$$

Discussion of the errors involved in the determination of the upper limit to the $N^{14}(n,p)C^{14}$ cross-section

The errors discussed in this section fall into three divisions; (1) those errors introduced by the assumption that certain quantities in the working equation were constants, (2) the random errors in track counting which are statistical in nature, and (3) those errors introduced as a consequence of the experimental technique.

Error in the value used for the cross-section of the $Li^6(n, \alpha)H^3$ reaction

Hughes[1] gives the thermal neutron cross-section of natural lithium as 71±1 barn and the cross-section of the $Li^6(n, \alpha)H^3$ reaction as 945 barns. Using an abundance for Li^6 of .0742 as given in the "Nuclear Data Sheets"[19], we have: .0742 x 945 = 70.119 . Therefore, the n-α reaction of Li^6 accounts for virtually all of the 71 barn cross-section of natural lithium and we may safely assume that the fractional error, $\varepsilon \frac{(\sigma_{Li^6})}{\sigma_{Li^6}}$, of the $Li^6(n, \alpha)H^3$ reaction is 1/71.

Error of the value used for the natural abundance of Li^6 and N^{14}

The "Nuclear Data Sheets"[19] lists the best values of the natural abundances of Li^6 and N^{14} as .0742 and .996337 respectively. They also state that there has been no variation in the abundance of nitrogen noted in gaseous samples and only a 1.4 per cent variation from the ratio of N^{14}/N^{15} of atmospheric nitrogen in the various compounds studied. The variation in the ratio of Li^6/Li^7 was 4.5 per cent in various samples studied. However, the largest factor in the lithium ratio variation was due to the inclusion of lithium taken from pitchblende in which it was felt appreciable n-α reactions had taken place.

There is a possibility that lithium and lithium compounds of recent manufacture do not contain the natural abundance of the lithium isotopes due to the extraction of Li^6 for other uses. However, the $LiNO_3$ used in this investigation is believed to have contained the

natural abundance of Li^6 since, by the appearance of the bottle from which it came, it seemed to be of old stock.

On the basis of these considerations, it is felt that no appreciable error in the determination of the upper limit for the nitrogen n-p cross-section will occur it we consider these abundances to be constant.

Random errors in the numbers of tracks counted

The standard deviation in the number of events which will occur when those events are random in nature is equal to the square root of the number counted. Therefore, the errors in the counts made of plates 1 and 3 and of the unexposed plate are:

$$\varepsilon\,(N_1^1) = \frac{\sqrt{3452}}{4.967} = \pm 12$$

$$\varepsilon\,(N_1^3) = \sqrt{49} = \pm 7$$

$$\varepsilon\,(N_{1b}^u) = \sqrt{19} = \pm 4$$

$$\varepsilon\,(N_s^1) = \frac{\sqrt{3627}}{4.967} = \pm 12$$

$$\varepsilon\,(N_s^3) = \sqrt{67} = \pm 8$$

$$\varepsilon\,(N_{sb}^u) = \sqrt{22} = \pm 5$$

Error in N_t^1 and in $N_p^1 + N_{sb}^1$ because of random errors in the numbers of tracks counted

It can be shown that the error in the sum or difference of a set of observed quantities is equal to the square root of the sum of the squares of the errors of each observable[20]. Since N_t^1 is given by:

$$N_t^1 = R/(R - 1) \quad (N_1^1 - N_1^3)$$

then
$$\varepsilon (N_t^1) = R/(R - 1) \sqrt{\varepsilon (N_1^1)^2 + \varepsilon (N_1^3)^2}$$

$$= \frac{47}{46} \sqrt{144 + 49} = \pm 14$$

Since $N_p^1 + N_{sb}^1$ is given by:

$$N_p^1 + N_{sb}^1 = N_s^1 - N_{sb}^u - N_t^1 ,$$

then
$$\varepsilon (N_p^1 + N_{sb}^1) = \sqrt{\varepsilon (N_s^1)^2 + \varepsilon (N_{sb}^u)^2 + \varepsilon (N_t^1)^2}$$

$$= \sqrt{144 + 25 + 225} = \pm 20$$

Error in the computed value of the upper limit of the $N^{14}(n, p)C^{14}$ cross-section

The fractional error of a derived quantity involving the multiplication or division of observables is given by the square root of the sum of the squares of the fractional error in each observable.[20] Therefore, the fractional error in the upper limit of the $N^{14}(n, p)C^{14}$ cross-section is given by:

$$\varepsilon (\sigma_{N^{14}}) = \sqrt{\frac{\varepsilon (N_p^1 + N_{sb}^1)^2}{(N_p^1 + N_{sb}^1)^2} + \frac{\varepsilon (N_t^1)^2}{(N_t^1)^2} + \frac{\varepsilon (\sigma_{Li^6})^2}{\sigma_{Li^6}^2}}$$

$$\varepsilon (\sigma_{N^{14}}) = \sqrt{\frac{400}{2304} + \frac{196}{435600} + \frac{1}{5041}} = \pm .174$$

Based on the fractional error as computed above, the error in the value of the upper limit of the n-p cross-section of nitrogen is ±1 barn.

Errors arising as a result of the experimental technique

In addition to the inability of the investigator to distinguish between the alpha particle tracks and the proton tracks (which is, without a doubt, the major source of error in this investigation), there are several other possible sources of error which arise from the experimental technique and are worthy of note. These are:

(a) The failure to get a true background count necessitated the computing of an upper limit to the cross-section rather than computing the value of the cross-section itself. Had a true background count been available, the investigation could have revealed the cross-section to within an accuracy of about fifty per cent.

(b) In counting the background on the unexposed plate, care had to be taken not to count aggregations of surface deposits having the appearance of short tracks. With the unexposed emulsion it was fairly easy to recognize these aggregations as surface deposit since they usually occured as a small section of the periphery of a ring. However, in an exposed plate with its attendant background, it is quite possible that the greater part of these rings might blend in with the background and the apparent track show up as undistinguishable from a true track. Consequently, the count of short tracks may have been high because of the inclusion of some of these "surface deposit tracks". Although no count of the number of "surface deposit tracks" per 1000 fields of view was made, it is estimated that there are about 4. This number is subject to great variation from area to area on an individual plate as well as from plate to plate depending

upon the plate's cleanliness. For each "surface deposit track" counted in 1000 fields of view, the computed value of the upper limit of the cross-section would have raised by about .1 barn.

(c) The moderate fog background of plates 1 and 3 may have obscured some of the short tracks. This may be particularly true of the proton tracks which have a larger grain spacing than the alpha particle tracks. It may be possible that no proton tracks were seen at all because of being lost in the fog background. The effect of losing a proton track in the background is to cause a decrease of about .1 barn in the computed value of the cross-section upper limit for each proton missed in 1000 fields of view.

(d) The targets for plates 1 and 3 were made by spraying a solution of water and the target compound onto a back-up plate. This method of target fabrication makes it rather unlikely that the target thickness will be of the designed value, or the same value, in any two targets. Consequently, the ratio, R, of the surface density of lithium on the target plate used in the exposure of plate 1 to the surface density on that target plate used in the exposure of plate 3 will not be the value used in the computation of the cross-section. However, since the targets were made in the same manner and with equivalent amounts of solution, it is estimated that the true ratio is not different from the value assumed by more than about 20 percent. A 20 percent error in the value of R would result in a cross-section differing in value from that computed (5 barns) by .16 barns.

V. SUMMARY AND CONCLUSIONS

Summary

An investigation was undertaken to determine the thermal neutron cross-section of the $N^{14}(n, p)C^{14}$ reaction using a nuclear emulsion technique. It was proposed to make this determination by exposing a target of lithium and nitrogen to a beam of thermal neutrons, recording in a nuclear emulsion the proton tracks of the nitrogen n-p reaction and the alpha particle and triton tracks of the lithium n-α reaction, and comparing the number of proton tracks per unit volume in the emulsion with the number of triton tracks per unit volume. A simple relationship exists between the number of tracks per unit volume and the cross-section; thus, the thermal neutron cross-section of the $N^{14}(n, p)C^{14}$ reaction is determined relative to the well-known cross-section of the $Li^{6}(n, \alpha)H^{3}$ reaction.

Although the theory was simple and the experimental method was straightforward, the investigation did not result in the accurate value of the cross-section that was hoped for. The major difficulty in the investigation was the inability to distinguish between the 6 micron proton tracks and the 6 micron alpha particle tracks. This resulted in extremely poor statistics and all efforts to improve the statistics were aborted by either excessive gamma radiation or excessive numbers of background tracks.

The investigation showed the upper limit of the $N^{14}(n, p)C^{14}$ reaction cross-section to be 5 ± 1 barns.

Comments on the use of nuclear emulsion techniques

The use of nuclear emulsion techniques in investigations of the kind with which this thesis was concerned has several distinct advantages over other techniques. These advantages make nuclear emulsions an attractive experimental tool despite the tedium of microscope work that attends their use. The nuclear emulsion is a relatively inexpensive method of collecting information on charged particle reactions. The emulsion records permanently the activity of all charged particles to which it is exposed from the time of its activation to the time of processing. This record is stored in the emulsion and is available to the researcher at any time he chooses to make use of it. The information yielded by the emulsion is extensive and includes such data as energies, angular correlations, frequency of event occurrance, etc..

Suggestions for the refinement of the technique used in this investigation and for further research.

The failure of this investigation to result in a precise value of the $N^{14}(n, p)C^{14}$ reaction cross-section should not, in itself, be taken as an indication of the inadvisability of employing nuclear emulsion techniques in the determination of cross-sections. It is felt that the relative low cost of employing nuclear emulsion techniques together with the large amount of information that can be recorded in only one plate make a continued search for a technique applicable to the determination of cross-sections quite reasonable. In this spirit, the following suggestions are made for refinements in the nuclear emul-

sion technique used in this investigation.

(a) The time of plate exposure and, hence, the number of tracks per field of view, was limited by the excessive gamma blackening that resulted from longer exposure times. The source of these gamma rays appeared to be the capture gamma rays of water in the area of the exposure chamber. If one designs the experiment to use the reactor beam hole for the incident neutron beam, then the plates can be exposed behind the concrete wall of the reactor pool and away from the capture gamma rays of water. This should result in the ability to expose the emulsions for any period of time desired.

The use of the beam hole will result in a longer incident beam tube length and, hence, a drop in the thermal neutron flux at the target. Therefore, one would be wise to investigate the possibility of using a larger diameter incident beam, a larger target, and the reactor core without the thermal column as the source of thermal neutrons.

(b) In the event that availability considerations obviate the use of the beam hole as the incident neutron beam tube and it is necessary to make exposures with the exposure chamber in the reactor pool as was done in this investigation, then it is suggested that a much larger chamber be used for plate exposures. A larger chamber would permit the inclusion of more lead shielding and the positioning of the nuclear emulsion further away from the incident neutron beam. With the additional lead shielding available, it may then be possible to expose the plates using the reactor core with a gain in thermal neutron flux of about 10^3 over that attainable at the face of the thermal

column. A larger thermal neutron flux, larger target, and larger incident beam tube would result in a greater number of tracks per field of view and, consequently, permit the investigation of smaller cross-sections than that of the $N^{14}(n, p)C^{14}$ reaction.

(c) To aid in the differentiation of the alpha particle and proton tracks, it is suggested that the investigator first expose plates to known sources of protons and alpha particles with energies close to those encountered in the nitrogen n-p reaction and the lithium n-α reaction.

The blackening of nuclear emulsions by gamma radiation makes the measurement of tracks difficult or impossible depending on the dosage received. An experiment designed to determine the gamma ray dose as a function of gamma ray energy that various type nuclear emulsions can be subjected to without rendering the recognition and measurement of tracks too difficult would be of some value. At present, this information is not available in the literature and it is necessary for each investigator to determine this limit for himself by time consuming trial and error.

BIBLIOGRAPHY

1. D. J. Hughes and J. A. Harvey, Neutron Cross-Sections, BNL 325, Second edition (1958)

2. A. R. Sattler, An Investigation of the Thermal Neutron Cross-Section for the Reaction $N^{14}(n, p)C^{14}$ using a Nuclear Emulsion Technique, thesis, The Pennsylvania State University (1959)

3. G. A. Bartholomew and P. J. Campion, Can. J. of Phys. 35, 1175 (1947)

4. C. La Pointe and F. Rasetti, Phys. Rev. 58, 554 (1940)

5. H. Lichtenberger, H. Fowler, and A. Wattenberg, ANL CP-781 (1943)

6. J. H. Coon and R. A. Nobles, Phys. Rev. 75, 1358 (1949)

7. F. O. Colmer and D. Littler, Proc. Phys. Soc. London A63, 1175 (1950)

8. D. E. Kline, Neutron Flux and Gamma Dose Rate Experiments with the Pennsylvania State University Research Reactor, June (1957)

9. E. S. Kenny, Private communication

10. H. A. Bethe and J. Ashkin, Experimental Nuclear Physics, vol. 1, Ed. by E. Segrè (John Wiley and Sons, Inc., New York, 1953)

11. F. Ajzenberg and T. Lauritsen, Rev. Mod. Phys. 27, 77 (1955)

12. J. Sharpe, Nuclear Radiation Detectors, (John Wiley and Sons, New York, 1955)

13. L. Vigneron, J. Phys. et Rad. 14, 145 (1953)

14. A. Beiser, Rev. Mod. Phys. 24, 273 (1952)

15. Y. Goldschmidt-Clermont, Ann. Rev. Nuc. Sci. 3, 141 (1953)

16. J. Rotblatt, Prog. Nuc. Phys. 1, 37 (1950)

17. C. F. Powell, P. H. Fowler, and D. H. Perkins, The Study of Elementary Particles by the Photographic Method, (Pergamon Press, New York, 1959)

18. Ilford Nuclear Emulsions, (An information paphlet on the characteristics of Ilford nuclear emulsions published by Ilford Research Laboratory, Ilford Limited, March 1961)

19. Nuclear Data Sheets, No. 1958-11-2 App 2, (National Academy of Science, National Research Council, Washington D. C.)

20. A. G. Worthing and J. Geffner, Treatment of Experimental Data, (John Wiley and Sons, New York, 1943)